UiO : Department of Physics
University of Oslo

A Novel Projection

Towards a Deeper Understanding of Mathematical Structures in the Composite Fermion Formalism

Knut Halvor Helland

Master's Thesis, Spring 2018

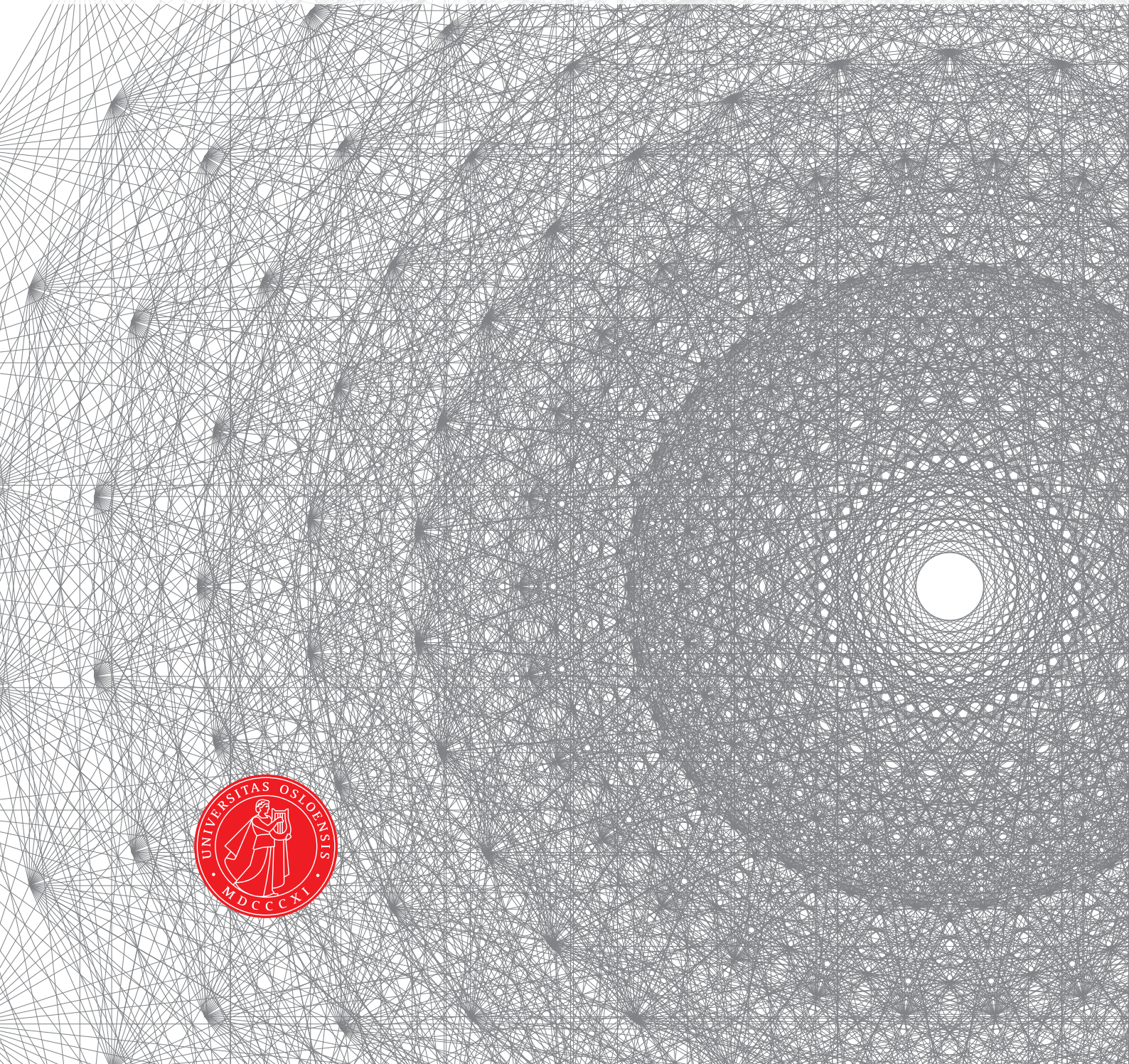

This master's thesis is submitted under the master's program *Physics*, with program option *Theoretical Physics*, at the Department of Physics, University of Oslo. The scope of the thesis is 60 credits.

The front page depicts a section of the root system of the exceptional Lie group E_8, projected into the plane. Lie groups were invented by the Norwegian mathematician Sophus Lie (1842–1899) to express symmetries in differential equations and today they play a central role in various parts of physics.

Abstract

Composite fermion (CF) wave functions are used to describe both a two dimensional electron gas in a strong magnetic field (the quantum Hall effect system) and rotating two dimensional atomic gases that can be either bosons or fermions. In this thesis a new method for projecting fermionic CF wave functions (here called method 3) to the lowest Landau level is investigated. The new projection is based on attaching a Jastrow factor to a bosonic CF wave function projected in the standard way. This will be compared to two other projection methods: method 1 or Girvin-Jach projection and method 2 or Jain-Kamilla projection. I compare the minimal cyclotron energy compact CF ground state candidates for the $\nabla^2\delta$ interaction both to each other and to the exact ground state found by numerical diagonalization for up to 8 particles. The conclusion is that the CF candidates typically are good approximations of the exact ground state, and that method 3 is almost as good as the other two at this.

An important motivation for method 3 is that it preserves linear dependencies from the bosonic states. The puzzle of linear dependencies is a part of CF theory that is not properly understood. Certain important results for low angular momentum states have been found for the bosonic case. Since method 3 works quite well in the cases tested here some of these results can be imported to the fermionic case. I have compared the linear dependencies among minimal cyclotron energy compact states for all three projection methods. If approximate linear dependencies are considered as proper linear dependencies then for all tested cases the same linear dependencies hold for all three projection methods, up to slightly different coefficients.

Acknowledgments

I would like to thank my supervisor Susanne Viefers for her kindness, encouragement and unending patience while guiding me through the process of learning, researching and writing about the composite fermion theory. I also thank Marius L. Meyer for so much help, especially with computer calculations and very many tricks and tips. Thanks to Vidar Skogvoll for many discussions about CF theory and additional help with the code. Finally I would like to thank everyone at Ad Undas, the study hall for students to practical for maths and not practical enough for *real* physics.

Contents

Chapter 1

Introduction

This thesis concerns a small corner of a corner of a corner of a large research field. This is perhaps in the nature of a modern master's thesis in physics (and to a lesser extent modern research in general). So it would probably be in the reader's interest if the topic is situated in the larger field before we start getting into the nitty-gritty details.

1.1 Topological Phases of Matter

The larger field is research into the topological phases of matter. The field developed in the late 20th century when it was discovered that in certain materials there existed phases and phase transitions that could not be explained by the current dominant theory, Landau symmetry breaking [1]. To my knowledge no one has been able to come up with a precise and non-technical explanation of what, exactly, constitutes a topological phase, and I won't be the first. I will settle for: topological phases are certain highly correlated quantum states with certain properties that are robust under small changes to the material.

These topological phases initially attracted interest at least in some part because they are *weird*. And, of course, weird things are interesting, because there is a good chance that the explanation of a weird phenomenon includes something *new* (if it could be explained entirely in terms of known science the phenomenon would probably not be considered so weird in the first place). After more than thirty years of research there is still a lot to be learned about topological phases, and much of the interest in the field is still pure curiosity.

There is, however, also a potential application: quantum computing. If universal quantum computers ever become realizable, it could constitute a revolution in computing as such computers are, theoretically, very very fast. One of the many problems to overcome is the handling of errors due to inevitable local perturbations to the state of the computer. Here certain topological phases may be helpful. Because topological phases are robust with respect to these kinds of perturbations they could be used to address the issue [2]. Of course the whole issue is a good deal more complicated than I make it out to be here, but quantum computing is not the topic of this thesis.

1.2 The Fractional Quantum Hall Effect and Low Dimensional Systems

One of the paradigms of topological phases is the fractional quantum Hall effect. This is a measurable effect that occurs for cold electrons in a strong magnetic field when confined to two dimensions. The effect shows up in different materials and is robust under small changes in purity and such. Each fraction corresponds to a topological phase. Much work has been done on the topic, some of which will be reviewed in the next chapter. It is an essential fact about the fractional quantum Hall effect that it occurs in two spatial dimensions (and one temporal). Many topological phases occur in such low dimensional systems [1]. Two dimensional systems also have the important quirk that particles there do not necessarily follow bosonic or fermionic statistics, but can rather follow a range of in-between statistics: they are *anyons* [3, 4]. When dealing with more than two anyons the interchange statistics can get pretty complicated. One way to think of the characterization of interchanges is through braids, where each braid equivalence class represents a different way to interchange particles. The braid group for two or more strands, representing two or more particles in this case, is infinite, so there are infinitely many different ways to interchange particles. How different braids manifest as different phases in the wave function depends on the nature of the system, but potentially each braid corresponds to a different phase. See figure 1.1 for some examples of braids on 4 strands. Many two dimensional topological phases, including fractional quantum Hall effect states, have anyonic quasiparticle excitations, which is both part of what makes them interesting and part of what makes them good candidates for quantum computing.

Another low dimensional system is a cold atom gas confined to two dimensions. It is theorized that if such a gas is rotated quickly enough, it should enter a topological phase comparable to those of the fractional quantum Hall effect, including having anyonic excitations. The atoms are electrically neutral and can be either bosons or fermions,but must interact in some way. It has proved difficult to realize such a phase, but in [5] it is claimed that it has been realized for gases of a few particles (less than 10) of ^{87}Rb, which are bosons.

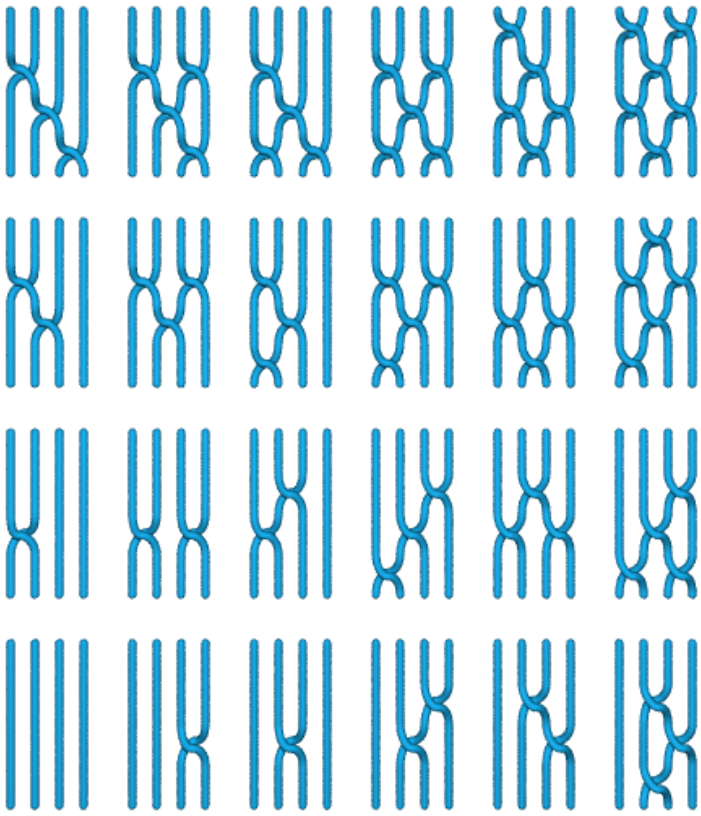

Figure 1.1: Representation of the permutation group S_4 as left-over-right 4 strand braids. The braid group on 4 strands B_4 is infinite, but can be generated by the three left-over-right braids that correspond to permutations. © Claudio Rocchini/CC-BY-2.5

1.3 This Thesis

This thesis concerns a set of wave functions called composite fermion wave functions that have been used to describe both the fractional quantum hall effect system of electrons in semiconductors and the cold atomic gas system that is intimately tied to it. I will study these wave functions as used to describe the system of a rapidly rotating cold fermionic gas of few particles with a short range interaction.

Part of the composite fermion formalism is a procedure called projection to the lowest Landau level. This procedure can be very computationally heavy and complicated, and there are certain mathematical structures of the procedure that are not very well understood. Projection introduces linear dependencies among states that were previously orthogonal [6]. This happens for both fermions and bosons, although the projection works slightly differently in the two cases, and research has been done into these linear dependencies for both, see for example [7, 8, 9, 10]. In particular, for certain bosonic low angular momentum states it has been possible to pick out states that form a basis after projection without actually doing the projecting [8, 9, 10].

In this thesis I will investigate an alternative method of projecting fermionic states to the lowest Landau level, which is computationally cheaper than the original method and connects immediately with the bosonic case. If the new method works well, its connection to the bosonic case will allow us to immediately import some of the important insights about the linear dependencies of the bosonic composite fermion wave functions to the fermionic case. I will also investigate how the linear dependencies among states projected by different methods compare to each other. I will use the original method, the new method and also a widely used alternative, based on a different simplification than "my" method.

Chapter 2 is a more detailed introduction to composite fermions, with the necessary background information on the quantum Hall effect. Chapter 3 introduces the new projection method and the tools I will use to investigate it, while the results are found in chapter 4.

Chapter 2

Background

This chapter provides background information to the investigation of a new projection method that is the topic of this thesis. I will first give a quick history of composite fermion wave functions, then I describe the quantum mechanical formalism of the problem. I also go through related work that informs the project.

2.1 History of Composite Fermion Wave Functions

2.1.1 The Hall Effect

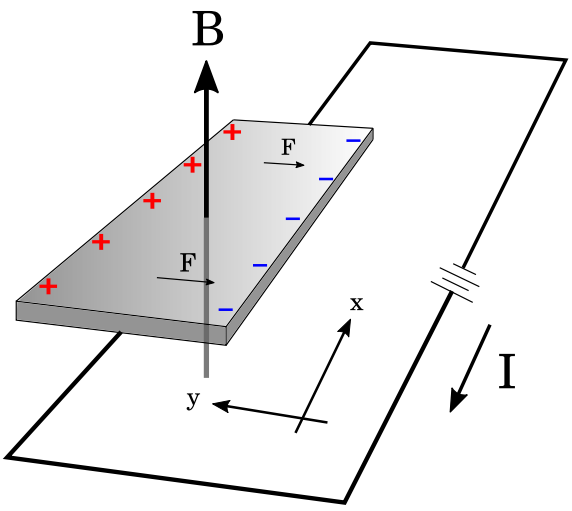

Figure 2.1: Illustration of the Hall effect. The Lorentz force from the magnetic field on the current pushes the electrons to one side, giving a transverse potential difference.

The Hall effect was discovered in 1879 by Edwin H. Hall [11]. He noticed that

Maxwell's equations implied that a current in a magnetic field transverse to the current should be subject to an electromagnetic force.

For a situation as in figure 2.1 with a current $\boldsymbol{I} = qv_x\boldsymbol{e_x}$ in a conductor and a magnetic field $\boldsymbol{B} = B\boldsymbol{e_z}$ Lorentz' law

$$\boldsymbol{F} = q\left(\boldsymbol{E} + \boldsymbol{v} \times \boldsymbol{B}\right) \tag{2.1}$$

implies a transverse force

$$F_y = qv_xB. \tag{2.2}$$

This force pushes the electrons in the $-y$-direction, leading to a difference in charge along the y-direction of the conductor. This in turn sets up an electric field E_y in the y-direction. When the force on the electrons due to E_y balances the force due to the magnetic field the situation is stable with a constant transverse electric field $E_y = E_H = v_xB$. It is useful to translate E_H into a resistivity by dividing by the current density in the x-direction $j_x = \rho q v_x$, where ρ is the number density of electrons. So the Hall-resistivity:

$$\rho_H = \frac{E_H}{j_x} = \frac{B}{\rho q}. \tag{2.3}$$

In two dimensions resistance and resistivity have the same dimensions, so rather than speak of the Hall resistivity we may speak of the Hall resistance:

$$R_H = \frac{B}{\rho q}. \tag{2.4}$$

2.1.2 The Quantum Hall Effect

In 1980 von Klitzing and his collaborators discovered the Quantum Hall Effect (QHE) [12]. It turns out that for two dimensional high-mobility conductors in low temperature and with high magnetic fields, the Hall resistance is not proportional to the strength of the magnetic field, but rather it is quantized in plateaus. Von Klitzing and his team discovered plateaus in the resistance of the form:

$$R_H = \frac{h}{Ne^2}, \tag{2.5}$$

where h is Planck's constant, e is the electron charge and N is an integer. This is the *integer quantum Hall effect* (IQHE). See figure 2.2 for illustration. In order to compare this to the classical Hall effect we define the *filling factor*:

$$\nu \equiv \frac{hc\rho}{Be}. \tag{2.6}$$

Now equation (2.4) may be rewritten as

$$R_H = \frac{1}{\nu}\frac{h}{e^2}. \tag{2.7}$$

So we may state the IQHE as: When the filling factor is close to an integer value, the Hall resistance acts as if the filling factor *is* that integer value.

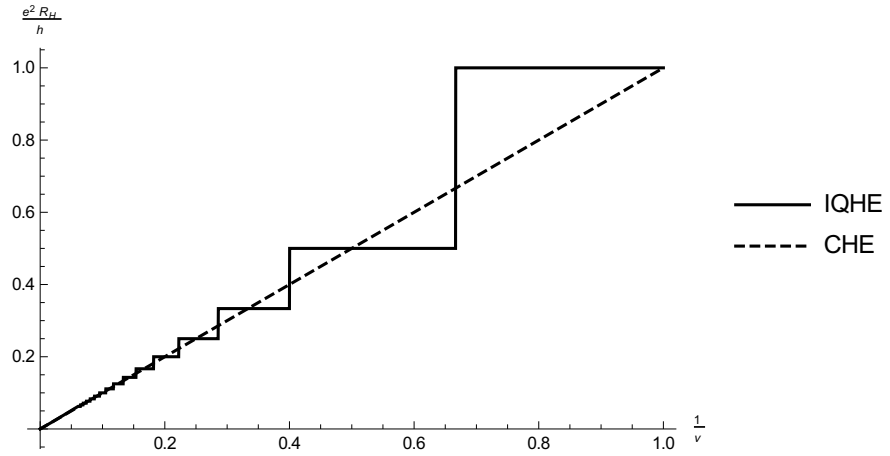

Figure 2.2: Illustration of the integer quantum hall effect. The dashed line is the classical Hall resistance, the solid line is an exaggeration of the observed plateaus in the resistance when ν is close to an integer.

In [13] Laughlin explained the IQHE qualitatively without taking interactions into account. Basically due to gaps in the energy levels and disorder in the sample, excess electrons or holes are trapped and cannot participate in conduction. The details are not important for our purposes.

Two years after von Klitzing's discovery Tsui and collaborators reported that they had discovered a new plateau in the Hall resistance at filling factor $\nu = 1/3$ [14]. Later more plateaus at fractions like $1/5, 1/7, 2/3, 2/5$ were discovered. In [15] the authors list more than 80 different fractions where plateaus have been discovered. This is the *fractional quantum Hall effect* (FQHE). While the IQHE could be understood in terms of non-interacting electrons, the FQHE could not. An explanation that accounted for interactions was needed.

2.1.3 The Laughlin Wave Function

To explain the $1/3$ FQHE Laughlin put forward in [16] the wave function

$$\Psi_{Laughlin} = \prod_{j<k} (z_j - z_k)^m \exp\left(-\frac{1}{4}\sum_i |z_i|^2\right), \tag{2.8}$$

where $z_k = x_k + iy_k$ in units of $\sqrt{\hbar c/eB}$ and m is an *odd* integer. The associated filling factor is $\nu = 1/m$. Laughlin calculated the exact ground state of the Coulomb interaction in the corresponding angular momentum subspace for 3 and 4 particles and a few different values of m and found that these states had a high overlap with the Laughlin state (2.8), indicating that (2.8) is very similar to the ground state. Laughlin also showed that the lowest lying bulk (meaning not edge) excitations of this state are quasiparticles that have fractional charge $1/m$ of the electron charge and also fractional statistics. By fractional statistics I mean that if the positions of two quasiparticles are exchanged counter clockwise, the wave function picks up a phase

$$\psi(\boldsymbol{r}_2, \boldsymbol{r}_1) = e^{i\pi\alpha}\psi(\boldsymbol{r}_1, \boldsymbol{r}_2), \tag{2.9}$$

with $\alpha = 1/m$. This means that the quasiparticles are neither fermions nor bosons but *anyons*. For fermions $\alpha = 1$ and for bosons $\alpha = 0$.

Laughlin showed that there is an energy gap from the ground state to the next lowest state for the $\nu = 1/m$ filling factors, i.e. the ground states are *incompressible*, which would explain why there is an FQHE for these fractions by the same reasoning as Laughlin's original explanation of the IQHE.

The Laughlin wave functions can explain the FQHE fractions $1/m$ and $1 - 1/m$ through particle-hole symmetry, but there are many more fractions that are not immediately explained in this way. There are several ways to extend this theory to account for more fractions. One of them is the *composite fermion formalism*.

2.1.4 Composite Fermion Wave Functions

In [17] Jain suggested a theory of the FQHE in terms of what he called *composite fermions* (CFs). In this picture electrons and vortices due to the magnetic field combine to make new composite particles, the CFs. These particles then "see" a weakened magnetic field and interact more weakly than electrons. The CFs then produce the IQHE, which manifests itself as the FQHE on the level of electrons. The theory includes a set of generalizations of the Laughlin states (2.8) of the form

$$\Psi_{CF} = \mathcal{P}_{LLL} \left\{ \Phi_{\nu^*} \prod_{j<k} (z_j - z_k)^{2p} \right\}, \tag{2.10}$$

where p is an integer, Φ_{ν^*} is a wave function of CFs with "CF filling factor" ν^* and $\mathcal{P}_{LLL}$ indicates projection to the lowest Landau level (LLL), which will be discussed in great detail later. This wave function gives an electron filling factor

$$\nu = \frac{\nu^*}{2p\nu^* \pm 1}, \tag{2.11}$$

and gives plateaus in the Hall resistance at fractions when ν^* is close to an integer. This CF theory explains many more fractions than the Laughlin states could, and also unifies the explanations of the IQHE and the FQHE. If we include "second order CFs" due to the interactions between the first order CFs giving rise to the same effect again, almost (but not quite) all of the observed fractions can be explained.

2.1.5 Rotating Gasses

The Hamiltonian for a particle in a rotating harmonic trap is structurally similar to that of a particle in a magnetic field [18]. In other words there is a mathematical relationship between the Quantum Hall system and the system of a rotating gas of atoms. This realization has led to much theoretical and experimental work investigating the connection between these two systems and which insights about the one system may be applied to the other [19]. Among this work has been to use CF wave functions to describe the rotating gas system. If the atoms in the gas are bosons the CF wave

functions are modified into

$$\Psi_{CF,bose} = \mathcal{P}_{LLL}\left\{\Phi_{\nu^*}\prod_{j<k}(z_j - z_k)^{2p+1}\right\}, \tag{2.12}$$

rather than (2.10).

It has turned out that these wave function have high overlaps with numerically calculated eigenstates for the rapidly rotating Bose-Einstein condensate (BEC) system, and much work has been done to investigate this. CF wave functions have also been extended to describe systems with two or more species of bosons [20, 21].

2.2 Composite Fermion Formalism

I now turn to a more technical description of the Composite Fermion formalism. In much of this section I follow the treatment in [22].

2.2.1 Geometry

I have described the QHE-system as electrons in a flat 2D piece of material with a transverse magnetic field. Indeed this is the natural experimental set up, however it is often convenient to use a geometry without edges for calculations. This is because edge effects can then be avoided, even in small systems.

There are several different geometries that capture the essential nature of the system, namely electrons confined to two dimensions with a transverse magnetic field. Jain does much of his work in the *spherical* geometry, where the electrons are confined to a sphere and the magnetic field is due to a magnetic monopole inside the sphere [22]. In his original paper on the IQHE Laughlin considered electrons on a cylinder [13]. Much work is also done on a torus [23]. In this thesis we will exclusively work with the *disc* geometry. Here the electrons are confined to flat surface that extends infinitely. In this geometry we do not avoid edge effects, as the particles end up in a droplet in the center of the disk, with an exponential tail. This geometry is also used in the work on rotating atomic gases referred to in the previous section.

2.2.2 Hamiltonians

For the QHE-system the relevant Hamiltonian is that of non-relativistic electrons confined to move in two dimensions in a perpendicular magnetic field. With the magnetic field as $\boldsymbol{B} = B\boldsymbol{e_z}$ the one particle Hamiltonian is

$$\hat{h}_{QHE} = \frac{1}{2m}\left(\hat{\boldsymbol{p}} + \frac{e}{c}\hat{\boldsymbol{A}}\right)^2, \tag{2.13}$$

where $B\boldsymbol{e_z} = \nabla \times \hat{\boldsymbol{A}}$. $\hat{\boldsymbol{A}}$ is not fully determined by this requirement, but rather there is *gauge freedom*. In the *symmetric gauge* $\hat{\boldsymbol{A}} = (B/2)(-\hat{y}, \hat{x}, 0)$. Then

$$\hat{h}_{QHE} = \frac{1}{2m}\left[\left(\hat{p}_x - \frac{eB}{2c}\hat{y}\right)^2 + \left(\hat{p}_y + \frac{eB}{2c}\hat{x}\right)^2\right]. \tag{2.14}$$

The one particle Hamiltonian for atoms in a harmonic trap of strength ω rotating with angular frequency Ω may be written

$$\hat{h}_{BEC} = \frac{\boldsymbol{p}^2}{2m} + \frac{1}{2}m\omega^2\boldsymbol{r}^2 - \Omega\hat{\ell}_z, \tag{2.15}$$

which can be rewritten as

$$\hat{h}_{BEC} = \frac{1}{2m}\left[(\hat{p}_x - m\omega\hat{y})^2 + (\hat{p}_y + m\omega\hat{x})^2\right] + \hat{h}_{HO} + (\omega - \Omega)\hat{\ell}_z, \tag{2.16}$$

where $\hat{h}_{HO}$ is the one dimensional harmonic oscillator in the z-direction. Comparing this with (2.14) we see that if we introduce $B_{eff} = 2m\omega c/e$ then

$$\hat{h}_{BEC} = \hat{h}_{QHE}(B_{eff}) + (\omega - \Omega)\hat{\ell}_z + \hat{h}_{HO}. \tag{2.17}$$

We will assume that the system is constrained to the lowest energy level of $\hat{h}_{HO}$, rendering the last term a constant that can be ignored. This constraint can be accomplished by making the oscillator frequency in the z-direction large. We will work in the limit $\omega \approx \Omega$, in which the term $(\omega - \Omega)\hat{\ell}_z$ is small. The important thing is that the energy from the term $(\omega - \Omega)\hat{\ell}_z$ is small enough to not mix the energy levels of $\hat{h}_{QHE}(B_{eff})$ [19]. We assume that there is no spin degree of freedom. In the electronic case this requires the magnetic field to be strong enough and the temperature low enough that all spins point in the same direction.

To treat the electronic and atomic picture simultaneously consider $\hat{h}_{QHE}$, from here on called just $\hat{h}$. If we introduce units $\ell_B = \sqrt{\hbar c/eB}$ ($\sqrt{\hbar/2\omega m}$) for length and $\hbar\omega_c = \hbar eB/mc$ ($2\hbar\omega$) for energy we may express the unitless version of the Hamiltonian as

$$\hat{h} = \frac{1}{2}\left[\left(-i\frac{\partial}{\partial x} - \frac{1}{2}\hat{y}\right)^2 + \left(-i\frac{\partial}{\partial y} + \frac{1}{2}\hat{x}\right)^2\right], \tag{2.18}$$

where h, x and y are now dimensionless. Introducing new coordinates

$$z = x + iy, \qquad \overline{z} = x - iy, \tag{2.19}$$

and notation

$$\partial = \frac{\partial}{\partial z}, \qquad \overline{\partial} = \frac{\partial}{\partial \overline{z}}, \tag{2.20}$$

we find

$$\hat{h} = \frac{1}{2}\left[-4\partial\overline{\partial} - \left(z\partial - \overline{z}\overline{\partial}\right) + \frac{1}{4}z\overline{z}\right]. \tag{2.21}$$

2.2.3 Landau Levels

The Hamiltonian (2.21) may be rewritten as

$$\hat{h} = \frac{1}{2}\left[\left(\frac{1}{2}\overline{z} - 2\partial\right)\left(\frac{1}{2}z + 2\overline{\partial}\right) + [\partial, z]\right], \tag{2.22}$$

or, if we define

$$a = \frac{1}{\sqrt{2}}\left(\frac{1}{2}z + 2\overline{\partial}\right), \tag{2.23}$$

then

$$\hat{h} = a^\dagger a + \frac{1}{2}. \tag{2.24}$$

Note that

$$[a, a^\dagger] = \frac{1}{2}\left([\partial, z] + [\overline{\partial}, \overline{z}]\right) = 1, \tag{2.25}$$

which means that if $\psi(z, \overline{z})$ is an eigenfunction of $\hat{h}$ with eigenvalue ϵ then $a^\dagger\psi(z)$ is also an eigenfunction with eigenvalue $\epsilon + 1$ and $a\psi(z, \overline{z})$ is an eigenfunction with eigenvalue $\epsilon - 1$. The function $\psi_0 = \exp(-z\overline{z}/4)/\sqrt{2\pi}$ has the properties $a\psi_0 = 0$ and $\hat{h}\psi_0 = \frac{1}{2}$ and thus defines the ground level. There is no normalizable function ψ_{max} for which $a^\dagger\psi_{max} = 0$ so there is no highest level. In sum we have found a set of (unnormalized) eigenfunctions

$$\psi_n = \left(a^\dagger\right)^n e^{-\frac{z\overline{z}}{4}} \tag{2.26}$$

with eigenvalues

$$E_n = n + \frac{1}{2}. \tag{2.27}$$

These energy levels are called the *Landau levels* (LLs).

2.2.4 Angular Momentum Eigenstates

The z-component of the angular momentum operator (the only relevant component in our system) is given in our units as

$$\hat{\ell} = \hbar\left(z\partial - \overline{z}\overline{\partial}\right). \tag{2.28}$$

If we move to the angular momentum in units of $\hbar$ the dimensionless ℓ is then

$$\hat{\ell} = \left(z\partial - \overline{z}\overline{\partial}\right). \tag{2.29}$$

If we define an operator b, similar to a, as

$$b = \frac{1}{\sqrt{2}}\left(\frac{1}{2}\overline{z} + 2\partial\right), \tag{2.30}$$

then

$$[b, b^\dagger] = 1 \tag{2.31}$$

and

$$\hat{\ell} = b^\dagger b - a^\dagger a. \tag{2.32}$$

As with a and $a^\dagger$, b and $b^\dagger$are ladder operators with a bottom rung ψ_0 with eigenvalue 0 and no top rung. Also

$$[b, a] = [b, a^\dagger] = 0, \tag{2.33}$$

so

$$[\hat{h}, \hat{\ell}] = 0. \tag{2.34}$$

Thus there exist simultaneous eigenfunctions for $\hat{h}$ and $\hat{\ell}$. We can construct these eigenfunctions by

$$\psi_{nm} = (b^\dagger)^{m+n}(a^\dagger)^n e^{-\frac{z\bar{z}}{4}}, \tag{2.35}$$

or in terms of associated Laguerre polynomials

$$L_n^m = \sum_{i=0}^{n} (-1)^i \binom{n+m}{n-i} \frac{x^i}{i!} \tag{2.36}$$

we have

$$\psi_{nm} = z^m L_n^m(z\bar{z}/2) e^{-\frac{z\bar{z}}{4}}, \tag{2.37}$$

which have eigenvalues

$$E_n = n + \frac{1}{2}, \quad n = 0, 1, 2 \ldots; \qquad \ell_m = m, \quad m = -n, -n+1, -n+2, \ldots \tag{2.38}$$

Note that in the *lowest* Landau level (LLL) where $n = 0$ the form of (2.37) is particularly simple:

$$\psi_m = (b^\dagger)^m e^{-\frac{z\bar{z}}{4}} = z^m e^{-\frac{z\bar{z}}{4}}. \tag{2.39}$$

This means that a general single particle state in the LLL may be given by a polynomial in only z times the exponential factor. In the LLL the operators $\hat{h}$ and $\hat{\ell}$ also take simple forms. Trivially $\hat{h}_{LLL} = 1/2$ adds only a constant, which we can ignore. Writing $p(z)$ for the polynomial part of the wave function we see

$$\begin{aligned} \hat{\ell}\psi_m &= (z\partial - \bar{z}\bar{\partial}) p(z) e^{-\frac{z\bar{z}}{4}} \\ &= (z\partial p(z)) e^{-\frac{z\bar{z}}{4}} - \frac{1}{4} p(z) z\bar{z} e^{-\frac{z\bar{z}}{4}} + \frac{1}{4} p(z) z\bar{z} e^{-\frac{z\bar{z}}{4}} \\ &= (z\partial p(z)) e^{-\frac{z\bar{z}}{4}}, \end{aligned} \tag{2.40}$$

so

$$\hat{\ell}_{LLL} = z\partial, \tag{2.41}$$

where it is understood that the derivative only acts on the polynomial part of the wave function.

2.2.5 Degeneracy and Filling Factor

As seen from (2.38) each Landau level is infinitely degenerate. However for each level there is a finite degeneracy per unit area. Consider the LLL. The absolute square of a LLL state $|\psi_m|^2$ is maximal at $r = \sqrt{2m}$. If we take this maximum as the position of the state then in a disk of radius R there are $\lfloor R^2/2 \rfloor$ states in the disk. The area of the disk is πR^2 so the degeneracy per unit area is (up to errors of order one due to ignoring the floor function) $1/2\pi$. As this is independent of R it must be constant. Although this looks independent of all parameters our length unit ℓ_B depends on the

magnetic field (or effective magnetic field). So with units the degeneracy per unit area is $eB/2\pi\hbar c$ $(m\omega/\pi\hbar)$. In fact this degeneracy per unit area is the same for all Landau levels [22].

Now we can introduce the filling factor from a different perspective: It is the number of Landau levels that would be filled if we put non-interacting fermions into this system. This is the 2D particle density divided by the degeneracy density:

$$\nu = \rho 2\pi = \frac{\rho 2\pi\hbar c}{eB} = \frac{\rho\pi\hbar}{m\omega}, \tag{2.42}$$

where ρ is the particle density given as a dimensionless number in units of $1/\ell_B^2$ and dimensionfully, respectively. We see that we have ended up with the same definition as in (2.6).

If the magnetic field (real or effective) is sufficiently strong compared to the particle density so that $\nu < 1$ and the temperature is very low then non-interacting particles would all be in the LLL. When we add interactions this is not strictly true, but if the interaction is weak enough compared to the density it is a reasonable approximation to focus only on the LLL.

2.2.6 Many Body LLL Wave Functions

For N particles the non interacting part of the LLL Hamiltonian is

$$\hat{H} = \sum_{i=1}^{N} \hat{h}_i = \frac{1}{2}N \tag{2.43}$$

and the total angular momentum operator is

$$\hat{L} = \sum_{i=1}^{N} \hat{\ell}_i = \sum_{i=1}^{N} z_i \partial_i. \tag{2.44}$$

Of course $[\hat{H}, \hat{L}] = 0$ still. As seen from the form of (2.39) in the LLL the many body wave functions are on the form

$$\psi_{LLL} = P(\{z\}) \exp\left(-\sum_i |z_i|^2/4 \right), \tag{2.45}$$

where $P(\{z\})$ is a polynomial in the z_is. If we choose to look at simultaneous eigenfunctions for $\hat{H}$ and $\hat{L}$, the polynomial must be *homogeneous*, i.e. the sum of the powers in each term must be the same and equal to total angular momentum L_{tot}. For bosons the polynomial must be totally symmetric under particle exchange, for fermions totally antisymmetric. Since the exponential factor $\exp\left(-\sum_i |z_i|^2/4\right)$ is present for all LLL wave functions I will usually suppress it to simplify notation.

All totally antisymmetric polynomials $P_A(\{z\})$ may be written as $\prod_{j<k}(z_j - z_k)P_S(\{z\})$, where $P_S(\{z\})$ is a totally *symmetric* polynomial [24]. The factor $\prod_{j<k}(z_j - z_k) \equiv \mathcal{J}$ is a Jastrow factor that will be called *the* Jastrow factor in this thesis. It is a homogeneous totally antisymmetric polynomial with total power in each term $N(N-1)/2$, which in our context means it carries an angular momentum $N(N-1)/2$.

A standard way to construct totally antisymmetric wave functions is a Slater determinant. A Slater determinant is a determinant of N single particle functions as functions of N coordinates z_i,

$$\begin{vmatrix} \psi_1(z_1,\overline{z}_1) & \psi_1(z_2,\overline{z}_2) & \dots & \psi_1(z_N,\overline{z}_N) \\ \psi_2(z_1,\overline{z}_1) & & & \\ \vdots & \ddots & & \vdots \\ \psi_N(z_1,\overline{z}_1) & \dots & & \psi_N(z_N,\overline{z}_N) \end{vmatrix}. \tag{2.46}$$

I will also use the notation

$$\mathcal{A}(\psi_1(z_1,\overline{z}_1)\psi_2(z_2,\overline{z}_2)\dots\psi_N(z_N,\overline{z}_N)), \tag{2.47}$$

where $\mathcal{A}$ is an antisymmetrization operator. Both these notations mean the same thing, explicitly

$$\sum_{\rho\in S_N}(-1)^{|\rho|}\psi_1(z_{\rho(1)},\overline{z}_{\rho(1)})\psi_2(z_{\rho(2)},\overline{z}_{\rho(2)})\dots\psi_N(z_{\rho(N)},\overline{z}_{\rho(N)}), \tag{2.48}$$

where S_N is the symmetric permutation group on N letters. I will also represent Slater determinants by occupation diagrams like this:

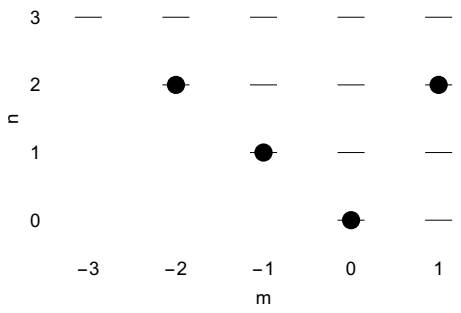

where the dashes represent possible single particle states and the dots represent the states that are occupied in the determinant.

The Jastrow factor is the antisymmetrization of the monomial $\prod_i z_i^{i-1}$, or the Slater determinant of the N lowest angular momentum LLL single particle eigenstates. The diagram representation of the Jastrow factor with $N = 4$ is

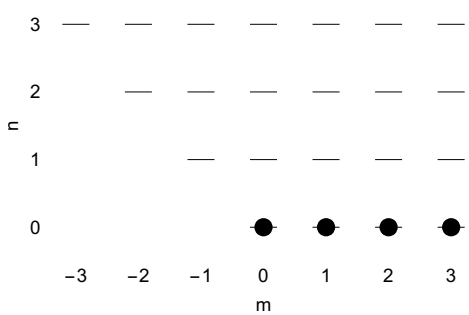

2.2.7 Composite Fermion Wave Functions (again)

In the composite fermion formalism the CFs have their own "internal" Landau levels in the reduced magnetic field, called Λ levels. A CF state is a Slater determinant Φ of single particle functions in these Λ levels. The CFs are not restricted to the lowest Λ level. Φ is then multiplied by p Jastrow factors, which attaches p vortices to each particle. For fermions p is even and for bosons it is odd. Finally as the final state is restricted to the lowest *Landau* level the state is projected to the LLL:

$$\psi_{CF} = \mathcal{P}_{LLL}\left\{\Phi \mathcal{J}^p\right\}. \tag{2.49}$$

In this thesis we will only look at states with minimal p, meaning $p = 2$ for fermions and $p = 1$ for bosons.

As an example of a CF state, if all the CFs are in the lowest Λ level and have minimal angular momentum, Φ is just another Jastrow factor. Then the wave function is already in the LLL and we recover the Laughlin wave function with $m = p + 1 = 3$. The CF filling factor here is $\nu^* = 1$ while the actual filling factor is $\nu = \nu^*/(p\nu^* + 1) = 1/(2 + 1) = 1/3$. To understand why, it is helpful to consider the diagram for the Jastrow factor

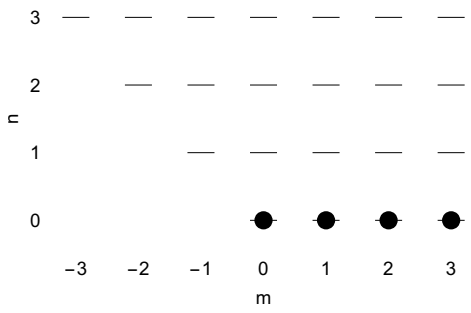

Considered as a total state this corresponds to a filling factor $\nu = 1$, graphically we see that the lowest level is filled from the left,and all other levels are empty. The $m = 3$ Laughlin state is the Jastrow factor cubed. It thus has thrice the angular momentum of the Jastrow factor, but is still entirely in the LLL. The state cannot be written as a Slater determinant, and so there is no proper diagram for the whole state, but vaguely we can represent the state with the diagram

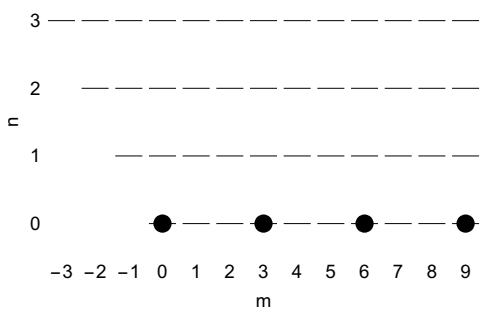

The increased angular momentum is manifested in spreading out the single particle states in angular momentum, resulting in the LLL being only $1/3$ filled.

If the Slater determinant is not completely made up of lowest Λ level states the projection to the LLL is more complicated. Let us first look at projecting a single particle state ψ_{nm} to the LLL [20]:

$$\langle \psi_{0m'} | \psi_{nm} \rangle = \int d^2z \, \overline{\psi}_{0m'}(z, \overline{z}) \psi_{nm}(z, \overline{z}). \tag{2.50}$$

A given term in this expression looks like

$$\int d^2z \, \overline{z}^{m'} z^{m+k} \overline{z}^k e^{-z\overline{z}/2}, \tag{2.51}$$

which may be rewritten

$$\int d^2z \, \overline{z}^{m'} z^{m+k} (-2\partial)^k e^{-z\overline{z}/2}, \tag{2.52}$$

integrating by parts k times gives

$$\int d^2z \, \overline{z}^{m'} \left[(2\partial)^k z^{m+k} \right] e^{-z\overline{z}/2}. \tag{2.53}$$

It seems that projecting $\psi_{m,n}(z, \overline{z})$ to the LLL is equivalent to pulling $\overline{z}$ to the left and then replacing $\overline{z} \to 2\partial$, where the derivative only acts on the polynomial part of the expression, not the exponential part. Introducing the notation $: \; :$ to indicate pulling derivatives to the left we can write

$$\mathcal{P}_{LLL} \{ \psi(z, \overline{z}) \} = : \psi(z, 2\partial) : . \tag{2.54}$$

This projection is formalized in [25], and also works on operators.

This implies that projecting a CF wave function to the LLL may be done by projecting the single particle states in the Slater determinant in this way, and letting the derivatives act also on the Jastrow factors. This projection method is known as Girvin-Jach projection, in this thesis I will call it projection method 1. In chapter 3 I will present two alternative projection methods, both of which are simplifications of the method presented here.

A CF wave function is determined by whether the basic particles are bosons or fermions, the projection method and the single particle states that go into the determinant. So to a large extent the differences between CF states lie in the Slater determinant part, so I will often represent CF states by for example the occupation diagram of the determinant.

2.3 Particle Interactions

So far we have considered only then non-interacting parts of the Hamiltonians. In the quantum Hall effect system, the basic particles are electrons that interact by the Coulomb interaction. In particular the FQHE may only be explained in terms of particle interactions, and trial wave functions like the Laughlin or CF wave functions are useful precisely because they are supposed to capture these interactions.

For the rotating gas system interactions are similarly essential, and using CF wave functions on this system is only relevant when the interaction is strong enough to matter. Here we will consider the basic particles of the gas to be electrically neutral atoms that interact by a short-range or contact interaction, but in general the particles could be charged and interact via the Coulomb interaction or some other repulsive interaction.

Let us first add a generic two body interaction term to the Hamiltonian we have been working with:

$$\hat{V} = \sum_{i<j} \hat{v}(|\boldsymbol{r}_i - \boldsymbol{r}_j|^2) = \sum_{i<j} \hat{v}((\overline{z}_i - \overline{z}_j)(z_i - z_j)). \tag{2.55}$$

The interaction depends only on the relative position of pairs of particles. Projecting this to the LLL we find

$$\hat{V} = \sum_{i<j} f(\partial_i - \partial_j) g(z_i - zj)), \tag{2.56}$$

where f and g depend on the form of $\hat{v}$. Consider potentials on the form

$$\hat{V} = g \sum_{i<j} \sum_{m=1}^{\infty} v_m (z_i - z_j)^m (\partial_i - \partial_j)^m, \tag{2.57}$$

where g is the strength of the interaction and v_m determines the form. This class of interactions is quite large and includes the Coulomb, δ and $\nabla^{2n}\delta$ interactions [26].

In the LLL the non-interacting part of the Hamiltonian only contributes a constant which we can ignore. Then,

$$\hat{H} = \hat{V}. \tag{2.58}$$

When $\hat{V}$ is on the form of equation (2.57) it commutes with $\hat{L}$:

$$\begin{aligned}
[\hat{V}, \hat{L}] &= \sum_{m,i<j} g v_m \sum_k [(z_i - z_j)^m (\partial_i - \partial_j)^m, z_k \partial_k] \\
&= \sum_{m,i<j} g v_m m (z_i - z_j)^{m-1} \\
&\qquad \times \left(\sum_k \left((z_i - z_j)\partial_k - z_k(\partial_i - \partial_j) \right) (\delta_{ik} - \delta_{jk}) \right) \\
&\qquad \times (\partial_i - \partial_j)^{m-1} \\
&= 0,
\end{aligned} \tag{2.59}$$

because the middle sum cancels. Then $\hat{V}$ separates into sections for a given L_{tot}, and there are energy eigenstates for each value.

For the atomic gas system there is an additional term $(\omega - \Omega)L_z$. We have assumed that this term is small, so to find the ground state it we should focus primarily on $\hat{V}$. However it is clear that additional angular momentum does contribute *some* energy so long as $\omega \neq \Omega$, so for two states with the same interaction energy the one with the lowest angular momentum has the lowest energy.

2.4 Translational Invariance and Center of Mass Angular Momentum

The total angular momentum operator in the LLL takes the form

$$\hat{L}_{LLL} = \sum_i z_i \partial_i. \tag{2.60}$$

A related operator is the LLL center of mass (COM) angular momentum:

$$\hat{L}_c = \frac{1}{N} \sum_{ij} z_i \partial_j = R\hat{D}_c, \tag{2.61}$$

where $R = \sum_i z_i/N$ is the COM coordinate, $\hat{D}_c = \sum_i \partial_i$ and all derivatives act only on the polynomial part of the wave function. For a wave function ψ with total angular momentum $L_{tot} = L^*$ and $\hat{D}_c\psi = 0$, which implies $L_c = 0$, there is a set of states

$$\psi' = R^l \psi, \tag{2.62}$$

with $L_c = l$ and $L_{tot} = L^* + l$. These states are called COM excitations.

Consider interactions on the form of (2.57). The commutator $[\hat{V}, R] = 0$:

$$\begin{aligned}
[\hat{V}, R] &= \sum_{m,i<j} g v_m \sum_k [(z_i - z_j)^m (\partial_i - \partial_j)^m, z_k] \\
&= \sum_{m,i<j} g v_m m (z_i - z_j)^m (\partial_i - \partial_j)^{m-1} \sum_k (\delta_{ik} - \delta_{jk}) \\
&= 0.
\end{aligned} \tag{2.63}$$

This means that for any eigenstate of $\hat{V}$ the COM excitations are also eigenstates with the same eigenvalue, but higher L_{tot}. This means that we can generate the whole set of eigenstates from the subset with $L_c = 0$.

A related concept to COM angular momentum is *translational invariance* (TI). In general a state $\psi(\{\boldsymbol{r}\})$ is TI if $\psi(\{\boldsymbol{r}\} + \boldsymbol{k}) = \psi(\{\boldsymbol{r}\})$, in other words the state does not change if all coordinates are changed by the same vector. No LLL wave function is TI in this sense, because the exponential factor is not TI. Therefore we instead define TI to mean invariant under a constant shift in only the polynomial part of the wave function: $p(\{z\} + k) \exp(-\sum_i |z_i|^2/2) = p(\{z\}) \exp(-\sum_i |z_i|^2/2)$.

The connection with COM angular momentum is that a state being TI is equivalent to having $L_c = 0$. To see this consider (following [27]) a translation operator

$$\hat{T}(k) = e^{-\boldsymbol{k} \cdot \sum_i \nabla_i}. \tag{2.64}$$

In two dimensions with our notation $\boldsymbol{k} \cdot \nabla = (k + \bar{k})(\partial + \bar{\partial})/2 + (k - \bar{k})(\partial - \bar{\partial})/2$. In the LLL we may disregard the $\bar{\partial}$ derivatives so we are left with $\boldsymbol{k} \cdot \nabla = k\partial$. This gives

$$\hat{T}(k) = e^{-k \sum_i \partial_i} = e^{-k\hat{D}_c}. \tag{2.65}$$

Clearly $[\hat{T}(k), \hat{D}_c] = 0$, so the operators have simultaneous eigenfunctions. Let ψ be such a simultaneous eigenfunction. If $\hat{T}(k)\psi = \psi$ then $\exp(-kD_c)\psi = \psi$ (where

D_c is the eigenvalue of $\hat{D}_c$), which means that $D_c = 0$. If $\hat{D}_c\psi = 0$ then $\hat{T}(k)\psi = \sum_n (-k\hat{D}_c)^n\psi/n! = \psi$, so ψ is TI. Thus TI is equivalent to $D_c = 0$, which is equivalent to $L_c = 0$. If a state is an eigenfunction of one operator but not the other it can be expanded in simultaneous eigenfunctions and the argument still holds.

In total this means that if we find only TI states we avoid the COM excitations.

2.5 Compact States

There is a special subset of CF states that is particularly interesting called *compact states*. Compact states may be characterized by their diagrams in the following way: *A state is compact if, for an occupied single particle state, there is no unoccupied state directly to the left or directly below it*. In other words the state diagram is filled from the left and from below. For example the state

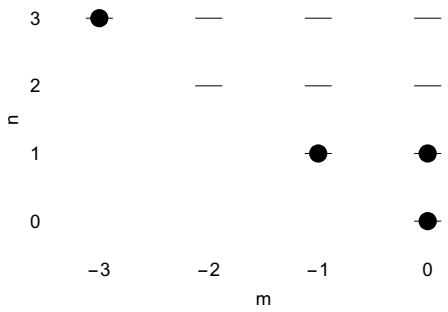

is compact, while the state

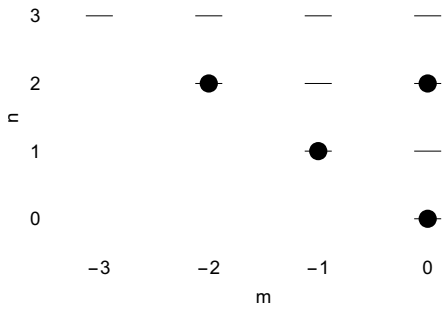

is not, because the occupied $n = 2, m = 0$ state has unoccupied states both to the left of and below it.

These compact states are good candidates for low energy states and are guaranteed to be translationally invariant. A reason to expect them to have low energy is that any non compact state can be turned into a compact state by moving the offending single particle states into the empty slots below or to the left. This procedure will reduce either the Λ-level (the CF energy level or CF cyclotron energy) or the angular momentum or both. In addition to this the projected Slater determinants of compact states may be written on a simple form, making them easier to deal with.

To see the simple form consider (following [20]) a column of a Slater determinant:

$$\begin{vmatrix} \psi_{n_1,m_1}(z,\overline{z}) \\ \vdots \\ \psi_{n_i,m_i}(z,\overline{z}) \\ \vdots \\ \psi_{n_N,m_N}(z,\overline{z}) \end{vmatrix}. \tag{2.66}$$

If this is a compact state, then for a given occupied single particle state $\psi_{n_i,m_i}(z,\overline{z})$ either $m_i = -n_i$, $n_i = 0$ or all $\psi_{n,m_i}(z,\overline{z})$ with $0 \leq n < n_i$ are also occupied. In the first case we note that $\psi_{n,-n} = z^{-n}L_n^{-n}(z\overline{z}/2) = z^{-n}(-1/2)^n(z\overline{z})^n/n! \propto \overline{z}^n$. We can ignore the normalization, so these single particle states have the very simple form $\overline{z}^n$. If $n = 0$ then the Laguerre polynomial is just a constant, and so we find the simple form z^m. For the third case we note first that the associated Laguerre polynomials $L_{n,m}$ have the property that the coefficient is nonzero for all powers from $\max(-m, 0)$ to n. We also note that row operations only change the Slater determinant by a constant, which does not matter here. Then starting from a single particle state $\psi_{n,-n}$ or $\psi_{0,m}$ we can eliminate all powers except the largest from the state $\psi_{n+1,-n}$ or $\psi_{1,m}$ by row operations, and continue up the chain to the top. Then each state can be written as $\psi_{m,n} \to z^{n+m}\overline{z}^n$. Thus our column may be written

$$\begin{vmatrix} z^{n_1+m_1}\overline{z}^{n_1} \\ \vdots \\ z^{n_i+m_i}\overline{z}^{n_i} \\ \vdots \\ z^{n_N+m_N}\overline{z}^{n_N} \end{vmatrix}. \tag{2.67}$$

Projecting to the LLL (and disregarding the factors of 2) $z^{n+m}\overline{z}^n \to \partial^n z^{n+m}$. This can be simplified by $[\partial, z] = 1$, which implies that

$$\partial^n z^{n+m} = \partial^{n-1} z^{m+n}\partial + (m+n)\partial^{n-1} z^{m+n-1}. \tag{2.68}$$

The second term is the state below, and can be eliminated. Moving one more:

$$\partial^{n-1} z^{m+n}\partial = \partial^{n-2} z^{m+n}\partial^2 + (m+n)\partial^{n-2} z^{m+n-1}\partial \tag{2.69}$$

the second term corresponds to moving one derivative to the right in the $n-1$ level, so it can also be eliminated. This pattern continues, so we can write $\partial^n z^{n+m} \to z^{n+m}\partial^n$. The column now looks like

$$\begin{vmatrix} z^{n_1+m_1}\partial^{n_1} \\ \vdots \\ z^{n_i+m_i}\partial^{n_i} \\ \vdots \\ z^{n_N+m_N}\partial^{n_N} \end{vmatrix}. \tag{2.70}$$

It was possible to write the state in this simple form because the diagram was filled from below.

Now we can show that compact states are translationally invariant. For a constant shift $z \to z + k$ the simple form state corresponding to $\psi_{n,m}$ transforms as $z^{n+m}\partial^n \to (z+k)^{n+m}\partial^n_{z+k}$. But derivatives are invariant under a constant shift so $\partial_{z+k} = \partial$. Then we have $(z+k)^{n+m}\partial^n = \sum_{i=0}^{n+m} \binom{n+m}{i} k^{n+m-i} z^i \partial^n$. The coefficients $\binom{n+m}{i} k^{n+m-i}$ are constants. If the state is compact, then for an occupied state $\psi_{n,m}$ also $\psi_{n,m-1}, \ldots, \psi_{n,-n}$ are occupied. Thus we have rows in the determinant with terms from $z^0\partial^n$ up to $z^i\partial^n$ for every i up to $n+m$. Then we can eliminate each term but the largest in each row by row operations, and are again left with

$$\begin{vmatrix} z^{n_1+m_1}\partial^{n_1} \\ \vdots \\ z^{n_i+m_i}\partial^{n_i} \\ \vdots \\ z^{n_N+m_N}\partial^{n_N} \end{vmatrix}. \tag{2.71}$$

So for compact states the determinant is TI. To see that the total state is TI we note that the Jastrow factor

$$\mathcal{J} = \prod_{j<k}(z_j - z_k) \tag{2.72}$$

is manifestly TI.

2.6 Multi Component Gases and Simple States

So far we have considered one component systems, where all the particles are identical. In the electronic case this is possible due to the spin degree of freedom being frozen out, and in the atomic case there are several ways to accomplish this. However it is of course also possible to not make this simplification and allow several species of identical particles. In the atomic case these species could for example be different isotopes or different spin states of the same isotope. In the work I will consider here there is no mechanism for switching between species, and all species considered follow the same statistics. Also I will assume that the interaction is homogeneous, meaning that it does not discriminate between particles of different species.

For a gas with M species of atoms with N_α atoms of species α let $z_{\alpha,i}$ be the coordinate of particle i of species α. The generalization of CF states to M species is

$$\mathcal{P}_{LLL}\left\{\left(\prod_\alpha \Phi_\alpha\right)\mathcal{J}^p\right\}, \tag{2.73}$$

where p is odd or even depending on the statistics of the particles (1 or 2 in this thesis), Φ_α is a Slater determinant of Λ level states in the coordinates $\{z_\alpha\}$, and $\mathcal{J}$ is the total Jastrow factor

$$\mathcal{J} = \prod_{\mu<\nu}(z_\mu - z_\nu), \tag{2.74}$$

where μ and ν are combined indices $\mu = (\alpha, i)$. If all the Slater determinants are compact, then the whole state is compact.

For multi species gases there is a subset of compact states called *simple states* [20, 21]. For simple states *all* the CF single particle states in *all* the Slater determinants are of the form $\psi_{n,-n}$. Single particle states in compact states may be written as $z^{n+m}\partial^n$ which for simple states reduces to only ∂^n.

For the single species gas with N particles there is only one possible simple nonzero state, with the N single particle states being the N lowest $\psi_{n,-n}$ type states. Any other state is zero because in the bosonic case the highest power of the derivative is higher than the highest power of z, and in the fermionic case because the total power of the polynomial will be too low to be antisymmetrizable. While this one state is (trivially) the ground state for its angular momentum, it is obviously untenable as a ground state candidate for all other angular momentum values.

For multi component gases there are many more possible simple states, all lying in the angular momentum ranges

$$0 \leq L_b \leq \sum_{\alpha<\beta} N_\alpha N_\beta, \tag{2.75}$$

where L_b is the angular momentum for bosons [21]. For fermions there is an extra$N(N-1)/2$ units of angular momentum due to the extra Jastrow factor. These states have been shown in numerical studies to be good candidates for the ground states of multi component bosonic gases in this low angular momentum range [20, 27, 21].

2.7 Linear dependencies in CF states

Slater determinants of orthogonal single particle functions are orthogonal so long as at least one of the occupied functions in one determinant is not occupied in the other. So, all the different Slater determinants of Λ level states in the CF wave functions are orthogonal, but the final projected CF wave functions are not necessarily orthogonal or even linearly independent [6].

In one sense this is obvious, because the space of CF Slater determinants at a given L_{tot} is infinite, while the LLL at the same L_{tot} is finite. That being said, there are finitely many Slater determinants that survive (end up as non-zero) projection to the LLL, and there are linear dependencies even among these states. These linear dependencies might point the way to insights about the nature of CFs or CF wave functions.

One approach to understanding these linear dependencies is to introduce an interaction between CFs. This approach is taken in [7], where a special interaction serves to eliminate certain linearly dependent states. On the interpretation of CFs as real particles it makes a lot of sense to consider an interaction between them, but the interaction suggested here is very strange. It is infinitely strong and only exists between certain CF excitations and holes, precisely those that give linearly dependent wave functions. Surely this interaction is an ad hoc inclusion in the theory that does not resolve the linear dependency puzzle so much as reframe it as a question of why the interaction has the strange form that it has.

Another approach is to consider only the mathematical structure of projecting a CF Slater determinant to the LLL. This approach does not depend on the interpretation of CFs, only on the formalism. The goal of such an approach is to find proper rules

for which linear dependencies are introduced by projecting. Realists about CFs may find such mathematical rules less satisfactory than a physical explanation in terms of an interaction, but on the other hand such rules would not be ad hoc in the way the interaction from [7] is, and may well be viewed as the explanation for the strange form of the interaction.

This mathematical approach is taken in the series [8, 9, 10], where the mathematical origins of all linear dependencies among bosonic M-species simple states are found. It is then possible to construct a basis for the subspace of simple states before projection to the LLL.

Though a complete generalization of this basis to all *compact* bosonic states has not yet been found, some headway has been made. In [8] an algorithm for identifying and reducing linear dependencies among compact bosonic states for one or two species of particles is identified. If we limit ourselves to the minimal cyclotron energy band of compact states the procedure turned out to eliminate all linear dependencies, at least for up to twelve particles of one or two species, producing a basis for this subspace.

2.8 From Bosons to Fermions

As mentioned in section 2.2.6 the structure of LLL wave functions means that bosonic wave functions must be a totally symmetric polynomial multiplied with an exponential factor, while fermionic wave functions must be a totally antisymmetric polynomial with the same exponential factor. Any totally antisymmetric polynomial in $\{z\}$ may be written as a totally symmetric polynomial multiplied with a Jastrow factor. This means that any fermionic wave function may be written as a bosonic wave function multiplied with the Jastrow factor and any bosonic wave function may be written as a fermionic wave function divided by the Jastrow factor.

$$\psi_{fermi} = \psi_{bose} \times \mathcal{J}, \qquad \psi_{bose} = \psi_{fermi}/\mathcal{J}. \tag{2.76}$$

It is natural to wonder what the relationship between these counterpart wave functions are. In particular it is interesting to know the relationship between the energies of the counterparts. For a harmonic interaction potential and a harmonic trap the counterpart of a bosonic interaction eigenstate is also an eigenstate, with only a constant shift in energy [28]. In [29] it is shown that a class of exact ground state wave functions for bosons found in [30] have a high overlap with the exact fermionic ground states after being transformed to fermionic wave functions by applying a Jastrow factor. According to [31] it is expected that this mapping gives good approximations to all LLL states, especially for high angular momenta and a low number of particles.

This procedure is of course applicable to CF wave functions. While one could go from fermions to bosons, it it probably more relevant to go the other way, from bosons to fermions. This is because for a given CF Slater determinant or set of determinants, it is considerably simpler to find the bosonic wave functions than the fermionic, due to there being one less Jastrow factor in the bosonic case. So we can find a fermionic wave function like so:

$$\psi_{fermi} = \mathcal{J}\psi_{CF,bose} = \mathcal{J}\mathcal{P}_{LLL}\left\{\Phi\mathcal{J}\right\}. \tag{2.77}$$

One may also look at this mapping as an alternative method of projecting a fermionic wave function to the LLL, where instead of directly projecting according to method 1, we first project the bosonic counterpart, then add the second Jastrow factor to the result. The aim of this thesis is to investigate this projection method.

Chapter 3

Formalism

This chapter describes, in some technical detail, the concepts and methods needed to produce the results in chapter 4. I first introduce three methods for projection to the lowest Landau level. The rest of the chapter is then devoted to technical details needed to study these methods.

3.1 Alternative methods for LLL projection

3.1.1 Method 1

As shown in section 2.2.7 the projection of a single particle state to the LLL is given by

$$\mathcal{P}_{LLL}\left\{\psi(z,\bar{z})\right\} =: \psi(z, 2\partial) : . \tag{3.1}$$

Extending this projection to many particle states simply amounts to projecting each coordinate individually. The partial derivatives commute, so it does not matter what order this is done in. For a fermionic CF state this becomes

$$\mathcal{P}^1_{LLL}\left\{\Phi(\{z\},\{\bar{z}\})\mathcal{J}^2(\{z\})\right\} =: \Phi(\{z\},\{2\partial\})\mathcal{J}^2(\{z\}) : , \tag{3.2}$$

the derivatives are pulled to the left and apply to the polynomial parts of the single particle functions in the Slater determinant and the Jastrow factors. This is projection method 1.

Projecting in this way is very computationally expensive, and the cost rises quickly with the number of particles N. Each Jastrow factor has $N!$ terms, as does the Slater determinant. So there are $(N!)^3$ terms, each containing several derivatives. Even though the differentiation can be done very efficiently this quickly becomes a huge calculation, so it would be good to simplify it.

While this projection method is in a sense the mathematically correct one, it is not necessarily "more correct" than any other projection method for our purposes. We are using CF wave functions as trial wave functions to find approximations of ground states. If we manage to find good wave functions the technicalities of the projection do not matter, only the result does. Nevertheless it is useful to consider this projection method as a starting point, as it was this projection method that was used to establish

that CF wave functions could describe the QHE system in the first place. As a secondary motivation it may be noted that to the extent that the realist interpretation of the unprojected CF wave functions should be meaningful at all there ought to be some reasonable mathematical relationship between the projected and unprojected wave functions.

3.1.2 Method 2

Our first alternative to projection method 1 is known as the Jain-Kamilla projection method, or method 2 here [32]. This is the most commonly used projection method in the literature. To see how it works, first note that we may write

$$\mathcal{J}^2 = \prod_{i<j}(z_i - z_j)^2 = \prod_i \prod_{j\neq i}(z_i - z_j) = \prod_i J_i, \tag{3.3}$$

where

$$J_i \equiv \prod_{j\neq i}(z_j - z_i), \tag{3.4}$$

where the product is over all js except i. Then an unprojected CF wave function may be written

$$\sum_{\rho\in S_N}(-1)^{|\rho|}\left(\prod_{i=1}^{N}\psi_i(z_{\rho(i)},\overline{z}_{\rho(i)})\right)\left(\prod_i J_i\right) = \sum_{\rho\in S_N}(-1)^{|\rho|}\left(\prod_{i=1}^{N}\psi_i(z_{\rho(i)},\overline{z}_{\rho(i)})J_{\rho(i)}\right), \tag{3.5}$$

we see that we can "bake" the Js into the determinant as

$$\begin{vmatrix} \psi_1(z_1,\overline{z}_1)J_1 & \psi_1(z_2,\overline{z}_2)J_2 & \dots & \psi_1(z_N,\overline{z}_N)J_N \\ \psi_2(z_1,\overline{z}_1)J_1 & & & \\ \vdots & \ddots & & \vdots \\ \psi_N(z_1,\overline{z}_1)J_1 & \dots & & \psi_N(z_N,\overline{z}_N)J_N \end{vmatrix}. \tag{3.6}$$

If we applied projection method 1 to this determinant the normal ordering would in effect pull the Js back out. Projection method 2 is to project each element of the determinant by projection method 1 individually:

$$\mathcal{P}^2_{LLL}\left\{\Phi\mathcal{J}^2\right\} = \begin{vmatrix} :\psi_1(z_1,2\partial_1)J_1: & \dots & :\psi_1(z_N,2\partial_N)J_N: \\ \vdots & \ddots & \vdots \\ :\psi_N(z_1,2\partial_1)J_1: & \dots & :\psi_N(z_N,2\partial_N)J_N: \end{vmatrix}, \tag{3.7}$$

where the derivatives are evaluated before expanding the determinant. Studies have shown that this projection method yields states that are very similar to those projected by method 1, and thus are about as good as those projected by method 1 [6, 22]. We will also confirm this in chapter 4.

There are N^2 elements in the matrix, and for each element there is a set of derivatives acting on 2^N terms. So compared to the $(N!)^3$ sets of derivatives in method 1

there are $2^N N^2$ sets. $(N!)^3$ grows a lot faster with N than $2^N N^2$, and so we expect method 2 to be faster for large N. This sort of analysis is not very exact, and the actual cost will depend on the details of the implementations of the projection methods. Nevertheless, it gives a rough idea of how costly the different methods are. Method 1 becomes very costly quite quickly, usually stalling out at around 10 particles. Method 2 however has been used to calculate wave functions with up to 100 particles [22].

3.1.3 Method 3

A second alternative is the projection method mentioned in section 2.8, here called method 3. The single particle functions in the Slater determinant are projected in the same way as for method 1, but rather than letting the derivatives act on both Jastrow factors they act only on one of them, with the other being unaffected by the projection:

$$\mathcal{P}^3_{LLL}\left\{\Phi\mathcal{J}^2\right\} = \mathcal{P}^1_{LLL}\left\{\Phi\mathcal{J}\right\}\mathcal{J} = \mathcal{J}:\Phi(\{z\},\{2\partial\})\mathcal{J}:\,. \tag{3.8}$$

To the best of my knowledge this method is new in that it has not been systematically tested in the literature. Exploring it is one of the main tasks in this thesis. Why this method? First of all it is expected to work. As explained in section 2.8 this projection method amounts to attaching a Jastrow factor to a bosonic CF state projected by method 1. This procedure has proved a good way to create good approximations of fermionic eigenstates from bosonic eigenstates [29, 31]. And numerical work has shown that compact bosonic CF states are good eigenstate candidates for the δ interaction for both one and more species of particles [19, 27, 21]. Therefore fermionic compact CF states found by projection method 3 ought to be good approximations of the eigenstates of $\nabla^2\delta$ interaction, the closest fermionic analogue to the δ interaction.

Secondly, this projection method preserves the linear dependencies between bosonic states. If

$$\mathcal{P}^{bose}_{LLL}\left\{\Phi_0\mathcal{J}\right\} = \sum_i c_i \mathcal{P}^{bose}_{LLL}\left\{\Phi_i\mathcal{J}\right\}, \tag{3.9}$$

then

$$\mathcal{P}^3_{LLL}\left\{\Phi_0\mathcal{J}^2\right\} = \sum_i c_i \mathcal{P}^3_{LLL}\left\{\Phi_i\mathcal{J}^2\right\}, \tag{3.10}$$

which cannot be said of the other projection methods. This property means that we can immediately apply any insights about the linear dependencies for bosonic states to fermionic states produced by method 3. In particular the basis for the full space of simple bosonic states found in [8, 9, 21] is a basis for the full space of simple fermionic states projected by method 3 if each basis element is multiplied with a Jastrow factor. If method 3 provides good eigenstate candidates we can use this to approximate the full spectrum with comparatively low computational cost. Simple states only exist for two or more species (except for the one at $L_b = 0$), while this thesis will only consider single species systems. However the work in [8] on linear dependencies of compact states applies to single species bosonic states, where it could produce a basis for the lowest cyclotron energy band of compact states for all tested numbers of particles, up to 12. I will discuss this more shortly.

Finally method 3 should be much cheaper computationally than method 1 as it reduces the number of terms to be differentiated by a factor of $N!$. Note however

that this still leaves $(N!)^2$ terms, which grows very quickly with N. The number of terms grows much faster than the number of terms for method 2, so we should not necessarily expect to be able to use method 3 for as large systems as method 2.

3.1.4 Numerical Experiments

I will perform two "numerical experiments" to compare these three projection methods. First I will look at how well the different methods can be used to approximate the LLL ground states of an interaction potential for small values of N and L_{tot}. Previous work has shown that methods 1 and 2 will typically give good approximations, while method 3 has to my knowledge never been tested in this way. Secondly I will examine the linear dependencies between the ground state candidates projected by the different methods. I will also perform the procedure for eliminating linear dependencies from compact states outlined in [8] to check that the linear dependencies I find correspond to those found by the procedure.

The rest of this chapter contains some essential concepts and techniques for these experiments. The results are given in chapter 4.

3.2 Overlap

I will need to compare states to see how similar they are and for this I will use the overlap:

$$O(\psi, \phi) \equiv \frac{|\langle\psi|\phi\rangle|}{\sqrt{|\langle\psi|\psi\rangle\langle\phi|\phi\rangle|}}. \tag{3.11}$$

This is a number between 0 and 1, with 1 indicating identity up to normalization and 0 indicating orthogonality. As such its interpretation is straightforward: the higher the overlap the more similar the two states are. It is however worth noting that the similarity measured by the overlap is a specific kind of similarity. Two states may share many important properties and still have a low or zero overlap, for example two states may have the same interaction energy yet still have zero overlap. So this measure is not the be all and end all, nevertheless it is useful and the standard way of reporting similarity between states in this field, from [16] and on.

It is sometimes helpful to look instead at the overlap squared:

$$O^2(\psi, \phi) = \frac{|\langle\psi|\phi\rangle|^2}{|\langle\psi|\psi\rangle\langle\phi|\phi\rangle|}. \tag{3.12}$$

These have the property that the sum of the square overlaps of any state ψ with all the eigenstates of a Hermitian operator ϕ_i must be equal to 1:

$$\sum_i O^2(\psi, \phi_i) = 1. \tag{3.13}$$

So the square overlap with an eigenstate is the "share" of that particular eigenstate in ψ, which is in my opinion easier to interpret than the direct overlaps. Nevertheless I will mostly use overlaps, as this is the standard which makes it easier to compare with other work. It is simple enough to square the values when needed.

3.3 Basis

To perform the numerical experiments it is useful to represent the wave functions in a basis. Here I present the one used for my computations. It is chosen because it simplifies some calculations and because it is easy to translate it to a corresponding basis for bosonic states.

Call the space of totally antisymmetric homogeneous polynomials in N variables with total degree L_{tot} $\mathbb{A}(N, L_{tot})$. The many fermion LLL angular momentum eigenstates are elements of $\mathbb{A}(N, L_{tot})$ multiplied with an exponential factor $\exp(-\sum_i |z_i|^2/4)$ that is the same in each case. So the Hilbert space for each part of the many-body Hamiltonian for fermions $\mathbb{H}_F(N, L_{tot})$ is isomorphic to the space of the polynomial part $\mathbb{A}(N, L_{tot})$. One orthogonal basis for this space is the set of antisymmetrized monomials where the powers are sorted partitions of L_{tot} into N different integers $\ell_i \geq 0$. Let us call this basis the monomial basis. The monomial basis set corresponds to the set of sets of N non-negative integers ℓ_i where

$$\ell_i > \ell_{i+1}, \qquad \sum_{i=1}^{N} \ell_i = L_{tot}. \tag{3.14}$$

For example the only ways to accomplish this for $N = 4$ and $L_{tot} = 10$ are $\{7,2,1,0\}$, $\{6,3,1,0\}$, $\{5,4,1,0\}$, $\{5,3,2,0\}$ and $\{4,3,2,1\}$. So the monomial basis when $N = 4$ and $L_{tot} = 10$ is

$$\left\{\mathcal{A}\left(z_1^7 z_2^2 z_3^1 z_4^0\right), \mathcal{A}\left(z_1^6 z_2^3 z_3^1 z_4^0\right), \mathcal{A}\left(z_1^5 z_2^4 z_3^1 z_4^0\right), \mathcal{A}\left(z_1^5 z_2^3 z_3^2 z_4^0\right), \mathcal{A}\left(z_1^4 z_2^3 z_3^2 z_4^1\right)\right\}. \tag{3.15}$$

Any other monomial either has the wrong total power or is equal to zero or equivalent to one of the above under antisymmetrization. Thus it should be clear that this basis spans $\mathbb{A}(4, 10)$, and in general the monomial basis for a given N and L_{tot} spans $\mathbb{A}(N, L_{tot})$.

To see that the basis elements are orthogonal consider the inner product of two of them:

$$\begin{aligned}\langle \psi_a | \psi_b \rangle &= \int \left(\prod_i d^2 z_i\right) \mathcal{A}\left(\prod_i \overline{z}_i^{\ell_{a,i}}\right) \mathcal{A}\left(\prod_i z_i^{\ell_{b,i}}\right) e^{-\sum_i |z_i|^2/2} \\ &= \sum_{\rho,\sigma \in S_N} (-1)^{|\rho|+|\sigma|} \prod_i \int d^2 z_i \left(\overline{z}_i^{\ell_{a,\rho(i)}} z_i^{\ell_{b,\sigma(i)}} e^{-|z_i|^2/2}\right).\end{aligned} \tag{3.16}$$

The integral

$$\begin{aligned}\int d^2 z\, \overline{z}^k z^l e^{-|z|^2/2} &= \int_0^{2\pi} \mathrm{d}\phi\, e^{i\pi(l-k)} \int_0^{\infty} \mathrm{d}r\, r^{k+l+1} e^{-r^2/2} \\ &= \delta_{lk} 2\pi 2^k k!\end{aligned} \tag{3.17}$$

so

$$\langle \psi_a | \psi_b \rangle = \sum_{\rho,\sigma \in S_N} (-1)^{|\rho|+|\sigma|} \prod_i \delta_{\ell_{a,\rho(i)} \ell_{b,\sigma(i)}} (2\pi) 2^{\ell_{\sigma(i)}} \ell_{\sigma(i)}! \tag{3.18}$$

The only way there can be a non-zero term is if there is a matching power in ψ_b for every power in ψ_a, so for $\psi_a \neq \psi_b$

$$\langle \psi_a | \psi_b \rangle = 0, \tag{3.19}$$

and the basis is orthogonal. To make the basis orthonormal we note

$$\langle \psi | \psi \rangle = N!(2\pi)^N 2^{L_{tot}} \prod_i \ell_i! \tag{3.20}$$

so the states may be normalized with a factor

$$\frac{1}{\sqrt{N!(2\pi)^2 2^{L_{tot}} \prod_i \ell_i!}}. \tag{3.21}$$

We can consider either finite monomial bases for each $\mathbb{A}(N, L_{tot})$ or an infinite basis for the whole space of antisymmetric polynomials $\mathbb{A} = \bigcup_{(N,L_{tot})} \mathbb{A}(N, L_{tot})$, either way the monomial basis is orthogonal.

Any polynomial in $\mathbb{A}(N, L_{tot})$ may be expressed as a totally symmetric polynomial multiplied with a Jastrow factor. This means that $\mathbb{A}(N, L_{tot})$ is isomorphic to the space of totally symmetric homogeneous polynomials in N variables with total degree $L_b = L_{tot} - N(N-1)/2$, $\mathbb{S}(N, L_b)$. This space is again related to the space of bosonic LLL angular momentum eigenstates by multiplication of the same exponential factor as for the fermions.

This means that the monomial basis for $\mathbb{A}(N, L_{tot})$ corresponds to a monomial basis for $\mathbb{S}(N, L_b)$, with each antisymmetric basis state corresponding to a symmetric basis state multiplied with a Jastrow factor. For example

$$\mathcal{A}\left(z_1^5 z_2^4 z_3^1 z_4^0\right) \leftrightarrow \mathcal{S}\left(z_1^2 z_2^2 z_3^0 z_4^0\right), \tag{3.22}$$

where $\mathcal{S}$ is a symmetrization operator. The Jastrow factor itself is represented as

$$\mathcal{A}\left(z_1^{N-1} z_2^{N-2} \dots z_N^0\right). \tag{3.23}$$

To translate between the bosonic and fermionic bases, we add or subtract the powers of the Jastrow factors to or from the original. This procedure depends on the powers being sorted.

There is no simple exact formula for the dimension of these spaces as functions of N and L, but there is an approximation. Just like each antisymmetric basis element corresponds to a partition of L_{tot} into N different non-negative integers, each symmetric basis element corresponds to a partition of L_b into N different or equal non-negative integers:

$$\ell_i \geq \ell_{i+1}, \qquad \sum_{i=1}^{N} \ell_i = L_b. \tag{3.24}$$

This again corresponds to a partition of L_b into N or fewer strictly positive integers, by padding with zeros. The problem of integer partitions into maximally N terms has

been studied and it has been shown (for example in [33]) that the number of partitions $p_N(L_b)$ is

$$p_N(L_b) = \frac{L_b^{N-1}}{N!(N-1)!} + \mathcal{O}\left(L_b^{N-2}\right). \tag{3.25}$$

By the isomorphisms outlined above this relation also holds for the dimensions of the $\mathbb{A}(N, L_{tot})$, $\mathbb{S}(N, L_b)$, $\mathbb{H}_F(N, L_{tot})$ and $\mathbb{H}_B(N, L_b)$ spaces.

This is not a particularly precise result for small Ls and Ns, but it tells us that for a fixed number of particles the number of dimensions grows quite quickly with the angular momentum as it becomes much larger than N.

There are of course other possible bases than the monomial bases, and there are also bases for subspaces, for example the TI subspace. The monomial bases were chosen first and foremost because they allow for many calculations to be done without ever expanding the antisymmetrization or symmetrization operators, which can make them much simpler.

3.4 The $\nabla^2\delta$ Interaction

While the electronic QHE system is usually studied with the full Coulomb interaction, systems of electrically neutral atomic boson systems are often studied with a δ interaction. The δ is a reasonably good approximation of the short range interactions between these particles. It only contributes to the energy when (loosely speaking) two particles are in the same position, i.e. when $z_i = z_j$. For fermions such an interaction can never contribute because the antisymmetric nature of the wave function makes it zero whenever $z_i = z_j$. So for the short range interactions between electrically neutral atomic fermion systems we need a different approximation.

According to [24] a short range interaction $\hat{V}(|\boldsymbol{r}|)$ may be expanded as

$$\hat{v}(|\boldsymbol{r}|) = \sum_{j=0}^{\infty} c_j b^{2j} \nabla^{2j} \delta^2(\boldsymbol{r}), \tag{3.26}$$

where b is the range. As shown in appendix A.1 for bosons only terms with even js contribute and for fermions only terms with odd js contribute. As $b \to 0$ only the first non vanishing term contributes for each kind of particles, so bosons are left with a δ interaction, while fermions are left with an interaction on the form

$$\hat{v}(\boldsymbol{r}) = g 2\pi \nabla^2 \delta^2(\boldsymbol{r}), \tag{3.27}$$

where g determines the strength of the interaction. In this thesis I will use this interaction with $g = 1$. In terms of coordinates z and $\bar{z}$ $\nabla^2 = 4\partial\bar{\partial}$ so the interaction is

$$\hat{v}(z) = 8\pi \partial\bar{\partial} \delta^2(z). \tag{3.28}$$

So the many body interaction term in the Hamiltonian is

$$\hat{V} = \sum_{i<j} \hat{v}(z_i - z_j) = \sum_{i<j} 8\pi \partial_i \bar{\partial}_i \delta^2(z_i - z_j). \tag{3.29}$$

The matrix elements of $\hat{V}$ in the monomial basis are given by

$$V_{ab} = \langle \psi_a | \hat{V} | \psi_b \rangle = \sum_{i<j} \int \left(\prod_{k=1}^{N} d^2 z_k \right) \overline{\psi}_a \psi_b v_{ij} \tag{3.30}$$

A generic term is of the form (dropping the normalization constants)

$$\int \left(\prod_{k=1}^{N} d^2 z_k \right) \mathcal{A}(\overline{z}_1^{\ell_{a,1}} \dots \overline{z}_N^{\ell_{a,N}}) \mathcal{A}(z_1^{\ell_{b,1}} \dots z_N^{\ell_{b,N}}) \exp\left(\sum_{i=1}^{N} -\frac{|z_i|^2}{2} \right) v_{ij} \tag{3.31}$$

or expanding the antisymmetrization operators

$$\sum_{\rho,\sigma \in S_N} (-1)^{|\rho|+|\sigma|} \int \left(\prod_{k=1}^{N} d^2 z_k \, \overline{z}_k^{\ell_{a,\rho(k)}} z_k^{\ell_{b,\sigma(k)}} e^{-\frac{|z_k|^2}{2}} \right) v_{ij}. \tag{3.32}$$

We can integrate out the non i and j coordinates by integral (3.17) noting that we only get contributions if for each ℓ_a except two there is a matching ℓ_b. These integrals add a constant that partially cancels the normalization constants of the basis functions. If τ is a (one of two) permutation that makes $\ell_{a,k} = \ell_{b,\tau(k)}$ for all $k \neq i, j$, then for a given ρ the only contributing terms are $\sigma = \rho \circ \tau$ and $\sigma = P_{ij} \circ \rho \circ \tau$, where P_{ij} is the permutation of the ith and jth coordinate:

$$\begin{aligned} \sum_{\rho} (-1)^{|\tau|} \int d^2 z_i d^2 z_j \, \overline{z}_i^{\ell_{a,\rho(i)}} \overline{z}_j^{\ell_{a,\rho(j)}} \left(z_i^{\ell_{b,\rho(\tau(i))}} z_j^{\ell_{b,\rho(\tau(j))}} - z_i^{\ell_{b,\rho(\tau(j))}} z_j^{\ell_{b,\rho(\tau(i))}} \right) \\ \times \exp\left(-\frac{|z_i|^2}{2} - \frac{|z_j|^2}{2} \right) \left(8\pi \partial_i \overline{\partial}_i \delta^2(z_i - z_j) \right). \end{aligned} \tag{3.33}$$

By integration by parts

$$\int d^2 z \, f(z,\overline{z}) \partial\overline{\partial}\delta(z) = \int d^2 z \, \left(\partial\overline{\partial} f(z,\overline{z}) \right) \delta(z). \tag{3.34}$$

Performing this transformation, evaluating the derivatives and integrating out the δ turns (3.33) into

$$\begin{aligned} &\sum_{\rho} (-1)^{|\tau|} 8\pi \left(\ell_{b,\rho(\tau(j))} - \ell_{b,\rho(\tau(i))} \right) \\ &\times \int d^2 z_i \Big(\ell_{a,\rho(j)} \overline{z}_i^{\ell_{a,\rho(i)} + \ell_{a,\rho(j)} - 1} z_i^{\ell_{b,\rho(\tau(i))} + \ell_{b,\rho(\tau(j))} - 1} \\ &\qquad - \frac{1}{2} \overline{z}_i^{\ell_{a,\rho(i)} + \ell_{a,\rho(j)}} z_i^{\ell_{b,\rho(\tau(i))} + \ell_{b,\rho(\tau(j))}} \Big) e^{-|z_i|^2} \end{aligned} \tag{3.35}$$

which gives

$$\begin{aligned} &\sum_{\rho} (-1)^{|\tau|} (2\pi)^2 \left(\ell_{a,\rho(j)} - \ell_{a,\rho(i)} \right) \left(\ell_{b,\rho(\tau(j))} - \ell_{b,\rho(\tau(i))} \right) \left(\ell_{a,\rho(i)} + \ell_{a,\rho(j)} - 1 \right)! \\ &\times \delta_{\ell_{a,\rho(j)} + \ell_{a,\rho(i)}, \ell_{b,\rho(\tau(i))} + \ell_{b,\rho(\tau(i))}}. \end{aligned} \tag{3.36}$$

Reinserting the normalization constants the total matrix element is then

$$V_{ab} = \sum_{i<j} \sum_{\rho} (-1)^{|\tau|} \frac{\left(\ell_{a,\rho(j)} - \ell_{a,\rho(i)}\right) \left(\ell_{b,\rho(\tau(j))} - \ell_{b,\rho(\tau(i))}\right) \left(\ell_{a,\rho(i)} + \ell_{a,\rho(j)} - 1\right)!}{N! 2^{\ell_{a,\rho(i)} + \ell_{a,\rho(j)}} \sqrt{\ell_{a,\rho(i)}! \ell_{a,\rho(j)}! \ell_{b,\rho(\tau(i))}! \ell_{b,\rho(\tau(j))}!}} \times \delta_{\ell_{a,\rho(j)} + \ell_{a,\rho(i)}, \ell_{b,\rho(\tau(i))} + \ell_{b,\rho(\tau(i))}} \tag{3.37}$$

We see that since the i, j-sum includes all possible pairs the permutations ρ only contribute a factor of $N!$:

$$V_{ab} = \sum_{i<j} (-1)^{|\tau|} \frac{\left(\ell_{a,j} - \ell_{a,i}\right) \left(\ell_{b,\tau(j)} - \ell_{b,\tau(i)}\right) \left(\ell_{a,i} + \ell_{a,j} - 1\right)!}{2^{\ell_{a,i} + \ell_{a,j}} \sqrt{\ell_{a,i}! \ell_{a,j}! \ell_{b,\tau(i)}! \ell_{b,\tau(j)}!}} \times \delta_{\ell_{a,j} + \ell_{a,i}, \ell_{b,\tau(i)} + \ell_{b,\tau(i)}} \tag{3.38}$$

For diagonal elements this simplifies to

$$V_{aa} = \sum_{i<j} \frac{\left(\ell_{a,j} - \ell_{a,i}\right)^2 \left(\ell_{a,i} + \ell_{a,j} - 1\right)!}{2^{\ell_{a,i} + \ell_{a,j}} \ell_{a,j}! \ell_{a,i}!}. \tag{3.39}$$

3.5 Exact Diagonalization

To see how well the CF ground state candidates approximate the exact ground state it is necessary to know the exact ground state. The Hilbert space $\mathbb{H}_F(N, L_{tot})$ for a given L_{tot} and N is finite, so we can find the complete interaction matrix $\boldsymbol{V}$ by equations (3.38) and (3.39). Then it is straightforward to find the interaction eigenstates and eigenvalues by numerically diagonalizing the matrix. This is called exact diagonalization, although it is only exact up to the numerical precision, about 10^{-14} here.

This is however very costly for large matrices. For an $n \times n$ - matrix most algorithms cost $\mathcal{O}(n^{2+\eta})$ operations where $0 \leq \eta \leq 1$ depending on things like the symmetry and sparsity of the matrix and of course the choice of algorithm. For large matrices personal computers will typically also run into memory issues, which will considerably slow down the calculation. For example with $N = 8$ particles and $L_{tot} = 84$, corresponding to the highest angular momentum compact states with eight particles , the dimension of the Hilbert space is 55974. So storing the matrix as a dense matrix of 32-bit numbers would take at least about 12 GB. Most personal computers don't have enough memory to store such a matrix, therefore diagonalizing it would be exceedingly slow.

The computational cost of exact diagonalization depends on $d_F(N, L_{tot})$ rather than the number of particles. So for high N low L_{tot} computations it is much faster than finding CF states by any projection method, while the cost of the three projection methods does not scale with L_{tot} in an obvious way, only N. Thus for relatively high L_{tot} and intermediary N it can be much faster to find CF states than to diagonalize directly.

3.6 Reduced Row Echelon Form of Matrices

One of the goals of this thesis is investigate the linear dependencies of CF states mentioned in section 2.7. In particular I want to look at how the new projection method 3 introduces these dependencies compared to methods 1 and 2. To do this I will want to display the dependencies among a set of vectors. One good way to do this is to look at the reduced row echelon form of the matrix formed by considering each vector a column. This form is unique and is found by performing row operations so that every zero row is to the bottom of the matrix and the first non-zero entry in each row is to the right of the first non-zero entry of the row above it, has value 1, and is the only non-zero entry in its column [34].

If the matrix is rank k, there will be k columns with only one non-zero element. The other columns, if there are any, can be read as coefficients for finding the original vector from the ones further to the left. For example: Let $\boldsymbol{v}$ and $\boldsymbol{u}$ be some linearly independent column vectors in $\mathbb{R}^3$. The matrix $(\boldsymbol{v}, \boldsymbol{u}, c_1\boldsymbol{v} + c_2\boldsymbol{u}, c_3\boldsymbol{u})$ has the reduced row echelon form

$$\begin{pmatrix} 1 & 0 & c_1 & 0 \\ 0 & 1 & c_2 & c_3 \\ 0 & 0 & 0 & 0 \end{pmatrix}. \tag{3.40}$$

3.7 Approximate Linear Dependency and Singular Values

Exact linear dependencies may be found and displayed by finding the reduced row echelon form of the matrix. But I will also want to look for *approximate* linear dependencies.

The notion of approximate linear dependency is a little unusual, so I will illustrate with an example. Consider the set of vectors in $\mathbb{R}^4$

$$\{\, (1,0,0,0), (0,1,0,0), (1,1,\epsilon,0) \,\}, \tag{3.41}$$

where $0 < \epsilon \ll 1$. Clearly this set is *not* linearly dependent, but nevertheless it seems clear that the smaller ϵ is, the closer the set is to being linearly dependent. One way to see this is to consider the overlap between the third vector ($|3\rangle$) and its projection onto the plane spanned by the first two vectors ($|3_{12}\rangle$):

$$O(|3\rangle\,, |3\rangle_{12}) = 1 - \frac{\epsilon^2}{4} + \mathcal{O}\left(\epsilon^4\right). \tag{3.42}$$

For small ϵs this number is very close to 1 and the two vectors are very close to being identical. It seems fair to say that we then have approximate linear dependency.

This approach is impractical for bigger sets of vectors and approximate linear dependencies that are more complicated. A more general approach is to look at *singular values*. An $(m \times n)$-matrix M over the complex numbers may be decomposed as

$$\boldsymbol{M} = \boldsymbol{U}\boldsymbol{\Sigma}\boldsymbol{V}^\dagger, \tag{3.43}$$

where $\boldsymbol{U}$ is a unitary $(m \times m)$-matrix, $\boldsymbol{V}$ is a unitary $(n \times n)$-matrix and $\boldsymbol{\Sigma}$ is a diagonal $(m \times n)$-matrix with the up to $\min(m, n)$ non-zero elements sorted in descending order [35, 36]. The number of non-zero singular values is the rank of $\boldsymbol{M}$. This may also be written as

$$\boldsymbol{M}\boldsymbol{V} = \boldsymbol{U}\boldsymbol{\Sigma}, \tag{3.44}$$

so letting $\boldsymbol{u}_i$ be the ith column of $\boldsymbol{U}$, $\boldsymbol{v}_i$ the ith column of $\boldsymbol{V}$ and σ_i the ith diagonal entry of $\boldsymbol{\Sigma}$

$$\boldsymbol{M}\boldsymbol{v}_i = \sigma_i \boldsymbol{u}_i. \tag{3.45}$$

Note the similarity to an eigenvalue equation and that

$$|\boldsymbol{M}\boldsymbol{v}_i|^2 = \sigma_i^2 \Leftrightarrow \boldsymbol{M}^\dagger \boldsymbol{M}\boldsymbol{v}_i = \sigma_i^2 \boldsymbol{v}_i. \tag{3.46}$$

The σs are the singular values of $\boldsymbol{M}$, they are the square roots of the eigenvalues of $\boldsymbol{M}^\dagger \boldsymbol{M}$.

For a rank k matrix $\boldsymbol{M}_k$ there are k non-zero singular values. For a perturbation $\boldsymbol{M} = \boldsymbol{M}_k + \boldsymbol{E}$ the remainder of the singular values are guaranteed to obey

$$\sum_{i=k+1} \sigma_i^2 \leq \sum_{ij} E_{ij}^2, \tag{3.47}$$

[37, 36]. This property makes singular values good tools for assessing approximate linear dependency. If some of the singular values are small then the elements of the matrix needed to perturb $\boldsymbol{M}$ to a matrix $\boldsymbol{M}_k$ for which they are zero are also small. Then we can say that $\boldsymbol{M}$ is approximately linearly dependent with the approximate dependencies in $\boldsymbol{M}$ corresponding to exact dependencies in $\boldsymbol{M}_k$.

Still it is important to take some care when using singular values to find approximate linear dependencies, because singular values scale with $\boldsymbol{M}$. Therefore one should use relative values of the singular values to find which ones are small in the sense that they indicate approximate linear dependence. I will also use normalized vectors to construct the matrices to make the differences easy to see, but the relative size is what counts.

The singular values for our example are

$$\begin{aligned} \sigma_1 &= \sqrt{2} - \frac{\epsilon^2}{8\sqrt{2}} + \mathcal{O}\left(\epsilon^4\right) \\ \sigma_2 &= 1 \\ \sigma_3 &= \frac{\epsilon}{2} + \mathcal{O}\left(\epsilon^3\right), \end{aligned} \tag{3.48}$$

where we clearly see that σ_3 is much smaller than the other values for small ϵ, as expected.

3.8 Ground State Candidates

I will examine as ground state candidates the sets of minimal cyclotron energy compact states. These are the compact states for a given N and L_{tot} that minimize the total

Λ-levels of the determinant. Let us for future reference call this set $\left\{\Phi^C_{min}\right\}$, with the subset for specific values of N and L $\left\{\Phi^C_{min,N,L}\right\}$. The reason to restrict the compact states to this subset is both that there are much fewer such states than compact states in general and that it seems reasonable, at least to the extent that the Composite Fermion interpretation is to be taken literally, that these are the lowest energy compact states.

I will look at these states for $N = 4$ to $N = 8$ particles, and for all angular momenta that are possible for these states. This is minimally $L_b = 0$ and maximally $L_b = N(N-1)$, but not all values in between are possible. Unfortunately I was not able to project the $N = 8$ states with projection method 2. This is because I ran into issues with the memory on my computer. I was not able to find an implementation that avoided this issue without being exceedingly slow, much slower than even my implementation of projection method 1. For $N = 8$ I also had to stop at $L_b = 44$. For $L_b = 45$ $d_8(45) = 17674$, but I again ran into memory issues when trying to diagonalize the 17674×17674-matrix, and could not complete the computation.

3.9 Eliminating Linear Dependencies of Compact States

Projection method 3 lets us directly import linear dependencies among bosonic states to the fermionic states. In [8] a procedure for finding linear dependencies among compact state determinants before projection is presented. Here I will briefly present the results from the article that pertain to single species compact states and the algorithm found by combining these results. For a more detailed treatment see [8]. I will use this algorithm to verify that it yields the same linear dependencies as projecting all determinants and finding linear dependencies directly in chapter 4.

There are two ways to identify the linear dependencies involved: *block permutation invariance* and *generalized translation invariance* of the Jastrow factor.

3.9.1 Block Permutation Invariance

Let us start with *blocks*, which are simplest to explain through occupation diagrams. Starting from the lowest row, the rows in a diagram may be partitioned into minimal sets of rows where the average occupancy is one. So for example in the following compact state

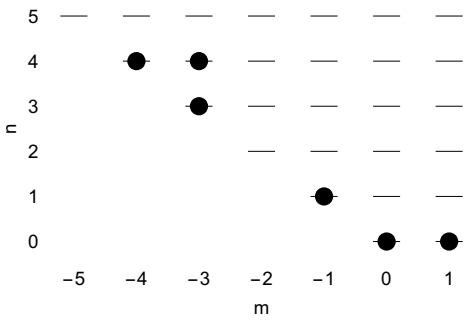

the rows 0, 1 and 2 form the first block, row 3 a second block and rows 4 and 5 a third.

Let each diagram correspond to a Slater determinant of single particle states $\phi_{nm} = z^{n+m}\partial^n$ applied to a *single* Jastrow factor. This corresponds to projecting a bosonic compact CF state into the LLL by method 1 or to the first step of a projecting a fermionic compact CF state to the LLL by method 3. Then it is proved in [8] that permuting the blocks does not change the bosonic state. Since attaching a Jastrow factor to each state does not change the linear dependencies also the fermionic states are left unchanged by a block permutation.

Our example diagram is then equivalent to all the following diagrams:

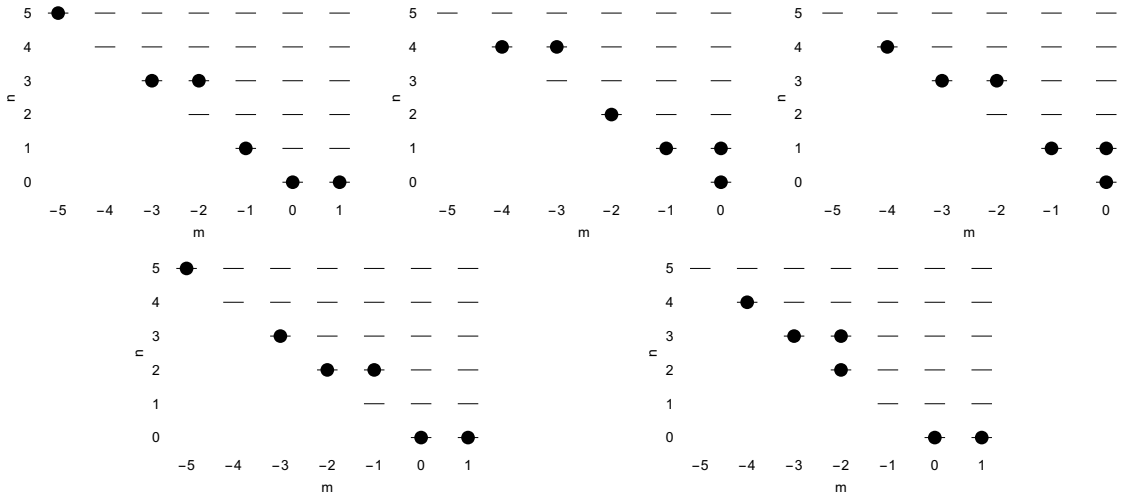

Of these the final one, corresponding to exchanging the first and third blocks of our example, is a compact state. Then these two compact determinants are equivalent, and we may discard one of them. All the other permutations break the rule that compact states should be filled from below, so they are not compact.

Remember that the single particle states here are ϕ_{nm} and *not* projected Λ-level orbitals $\mathcal{P}_{LLL}\{\psi_{nm}\} =: z^m L_m(z\partial):$. The association $\phi_{nm} \leftrightarrow \mathcal{P}_{LLL}\{\psi_{nm}\}$ only holds for compact states, so the permuted non-compact states are not the same as the CF states with the same diagram. Let us call these non compact states χ_i. Even though they are not CF states they can be useful to us, as we shall see.

3.9.2 Generalized Translation Invariance

In section 2.4 I explained that a state being translationally invariant is equivalent to the state having eigenvalue zero for the operator $\hat{D}_c = \sum_i \partial_i$. Compact states are TI, so they are zero under this operator and the same goes for Jastrow factors. A state has *generalized* translational invariance if it is zero under the operator

$$\hat{D}_a \equiv \sum_i \partial_i^a, \tag{3.49}$$

where a is an integer ≥ 1. Compact states do not have this property generally, but the Jastrow factor does. To see this, we first note that $\hat{D}_a$ is symmetric while $\mathcal{J}$ is antisymmetric, so $\hat{D}_a\mathcal{J}$ is antisymmetric. Next we note that a generic term in $\hat{D}_a\mathcal{J}$ looks like

$$\partial_i^a \prod_{j=1}^{N} z_j^{\rho(j)-1}. \tag{3.50}$$

If $a > \rho(i) - 1$ the term is zero and all is well. If instead $a \leq \rho(i) - 1$ there are two coordinates with power $\rho(i) - 1 - a$. But then the antisymmetry ensures that the term is canceled by the term with the two equal powers exchanged. Thus $\hat{D}_a \mathcal{J} = 0$.

To exploit this note that for a projected compact Slater determinant Φ

$$\begin{aligned}
\Phi \hat{D}_a &= \left(\sum_{\rho \in S_N} (-1)^{|\rho|} \prod_{i=1}^{N} z_k^{n_{\rho(k)} + m_{\rho(k)}} \partial_i^{n_{\rho(k)}} \right) \left(\sum_{j=1}^{N} \partial_j^a \right) \\
&= \sum_{j=1}^{N} \left(\sum_{\rho \in S_N} (-1)^{|\rho|} z_j^{(n_{\rho(j)} + a) + (m_{\rho(j)} - a)} \partial_j^{n_{\rho(j)} + a} \prod_{i \neq j} z_k^{n_{\rho(k)} + m_{\rho(k)}} \partial_i^{n_{\rho(k)}} \right) \\
&= \sum_{j=1}^{N} \Phi_j^a,
\end{aligned} \tag{3.51}$$

where Φ_j^a is the determinant Φ with the jth single particle state ϕ_{n_j, m_j} replaced with $\phi_{n_j + a, m_j - a}$. In diagram terms this corresponds to moving one state a spots up and to the left.

When thinking of states in terms of diagrams the single particle states are not ordered, so some care is needed to determine the sign of each term here. For example by choosing a base ordering and figuring out the signature of the permutation needed to reorder the Φ_i^a determinant into this ordering. As with block permutations some of the Φ_i^a will be compact,some will be unknown non compact functions χ_i, and some will be automatically zero if two particles occupy the same single particle state or if the maximal n is higher than $N - 1$. If a χ_i found here is a block permutation of a compact state, we can replace the χ_i with the compact state.

Now we can see the relation

$$\Phi \hat{D}_a \mathcal{J} = \sum_{i=1}^{N} \Phi_i^a \mathcal{J} = 0. \tag{3.52}$$

3.9.3 Combined Algorithm

By combining these results we find the following algorithm to reduce linear dependencies. Let $\left\{ \Phi^C_{K,N,L} \right\}$ be the set of compact determinants with N particles, total cyclotron energy $K = \sum_i n_i$ and bosonic angular momentum $L = \sum_i m_i + N(N-1)/2$. The algorithm is

1. Find $\left\{ \Phi^C_{K,N,L} \right\}$.
2. Delete determinants that are block permutations of other determinants.
3. For all $a = 1, 2, \ldots, \min(K, N-1)$:
   (a) Find $\left\{ \Phi^C_{K-a,N,L+a} \right\}$.
   (b) For all $\Phi \in \left\{ \Phi^C_{K-a,N,L+a} \right\}$ find all Φ_i^a and relations (3.52).

(c) If Φ_i^a is a block permutation of one of the remaining determinants in $\left\{ \Phi^C_{K,N,L} \right\}$ replace Φ_i^a with the one from $\left\{ \Phi^C_{K,N,L} \right\}$ in the relations.

4. Combining the relations found by (3.52), reduce as many of the remaining χ_is as possible.

5. Use the remaining relations with no χ_is to reduce $\left\{ \Phi^C_{K,N,L} \right\}$ further.

This algorithm has been tested for minimal K states up to 12 particles. In all cases all the linear dependencies are eliminated and we are left with a basis for the subspace spanned by $\left\{ \Phi^C_{min,N,L} \right\}$ [8].

Chapter 4

Results

In chapter 3 I described two "numerical experiments" meant to investigate projection method 3. In this chapter I collect and investigate the results of the experiments. First I wanted to see how good projection method 3 is at producing ground state candidates, both by comparing the method 3 candidates to the exact ground states and to the methods 1 and 2 candidates. These comparisons serve to determine if method 3 is a viable CF projection method, and are presented in section 4.1.

One of the main motivations behind projection method 3 is to better understand the linear dependency puzzle of CF wave functions, as described in chapter 2. As mentioned significant results have been found for the linear dependencies of *bosonic* CF wave functions. The fermionic projection method 3 preserves the bosonic linear dependencies, so using it we can immediately import insights about the bosonic case to the fermionic case. It is therefore interesting to see how the linear dependencies among the method 3 wave functions compare to those for methods 1 and 2. I present this in section 4.2.

4.1 Comparison of CF states with Exact Ground States

I have projected the minimal cyclotron energy compact states $\left\{\Phi^{C}_{min}\right\}$ for $N = 4-7$ with all three projection methods and up to $L = 44$ for $N = 8$ with methods 1 and 3. I have diagonalized the $\nabla^2\delta$ interaction for these N, L combinations in both the entire Hilbert space $\mathbb{H}_F(N, L)$ and the subspace spanned by the projected CF candidates. This produces exact eigenvalues and eigenvectors and CF ground state candidates, respectively. I will investigate how well the CF candidate states compare to the ground state first by considering the overlaps, and then by considering the energies.

4.1.1 Overlaps

Tables 4.1–4.5 show the overlaps of the ground state candidates with the exact TI ground state for four to eight particles, all possible angular momenta for compact states and all three projection methods. They also contain the overlaps among the candidates.

First of all some sanity checks: The number if ways to partition 0 into N non-negative integers is $d_N(0) = 1$ (N zeros), so the Hilbert space for N fermions with $L_{tot} = N(N-1)/2$, $\mathbb{H}_F(N, N(N-1)/2)$, is one dimensional. The overlap of any two states in this space must then be exactly 1, so in particular the overlaps of our ground state candidates with the exact ground state must be exactly 1. From the tables our candidates all check this box.

Next $d_N(1) = 1$, but this state must be the center of mass excitation of the $L_b = 0$ state, so it is not TI, and therefore there is no compact CF state here. $d_N(2) = 2$ for $N \geq 2$. Again there is a COM excitation, removing this we are left with the TI subspace which must then be one dimensional. Again any two states must have overlap 1. Again we note that this holds for all our examples. Finally $d_N(3) = 3$ for $N \geq 3$, which includes *two* COM excitations, and the TI subspace is one dimensional. The overlaps are all 1 here also, as they must be.

On the other end of the angular momentum spectrum, for $L_b = N(N-1)$ there is exactly one compact Slater determinant, the Jastrow factor. As mentioned the Jastrow factor is already in the LLL so all three projection methods leave it be. Thus the three projection methods all make the same state: the $1/3$ Laughlin state. This means that the overlaps among the candidates must be 1. Furthermore given Laughlin's work it would be very surprising if the overlap with the ground state were not quite high, and in fact a previous study of the $\nabla^2\delta$ interaction has shown that it is the exact ground state, not only for $L_b = N(N-1)$ but in the whole TI subspace for any angular momentum [24]. Again our candidates pass the test, as they all have overlap exactly 1 for $L_b = N(N-1)$ both among each other and with the exact ground state.

Table 4.1: Overlaps between the CF ground state candidates produced with projection methods 1, 2 and 3 and the exact ground state e for $N = 4$ particles. L is the bosonic angular momentum, related to total angular momentum as $L_{tot} = L + N(N-1)/2$.

L	$O(e,1)$	$O(e,2)$	$O(e,3)$	$O(1,2)$	$O(1,3)$	$O(2,3)$
0	1.000	1.000	1.000	1.000	1.000	1.000
2	1.000	1.000	1.000	1.000	1.000	1.000
3	1.000	1.000	1.000	1.000	1.000	1.000
4	0.998	0.999	0.990	1.000	0.997	0.996
6	0.984	0.985	0.982	1.000	1.000	0.998
7	1.000	1.000	1.000	1.000	1.000	1.000
8	0.991	0.991	0.991	1.000	1.000	1.000
12	1.000	1.000	1.000	1.000	1.000	1.000

Let us examine the other states in these tables. For 4 particles, table 4.1, there are four values of L_b that are not covered by the checks above. All of these overlaps are very high at 0.98 or above. The overlaps among the candidates are even higher. For $L_b = 4$ and 6 projection method 2 gives the highest overlap with the ground state, demonstrating that method 1 is not *always* the best, although the method 1 and method 2 candidates are very similar with overlap 1.000 to our accuracy. Method 3 gives the worst overlap here, with the difference in the third digit. For $L_b = 7$ and 8 all methods give the same overlap.

Table 4.2: Overlaps between the CF ground state candidates produced with projection methods 1, 2 and 3 and the exact ground state e for $N = 5$ particles. L is the bosonic angular momentum, related to total angular momentum as $L_{tot} = L + N(N-1)/2$.

L	$O(e,1)$	$O(e,2)$	$O(e,3)$	$O(1,2)$	$O(1,3)$	$O(2,3)$
0	1.000	1.000	1.000	1.000	1.000	1.000
2	1.000	1.000	1.000	1.000	1.000	1.000
3	1.000	1.000	1.000	1.000	1.000	1.000
4	0.998	0.999	0.989	1.000	0.996	0.995
5	0.995	0.996	0.976	1.000	0.993	0.991
6	0.932	0.931	0.931	1.000	1.000	1.000
7	0.988	0.988	0.988	1.000	1.000	1.000
8	0.989	0.984	0.981	0.999	0.997	0.997
9	0.954	0.953	0.966	1.000	0.992	0.991
10	0.965	0.964	0.950	1.000	0.997	0.997
11	0.421	0.421	0.421	1.000	1.000	1.000
12	0.974	0.974	0.974	1.000	1.000	0.999
13	0.803	0.803	0.803	1.000	1.000	1.000
14	0.256	0.256	0.256	1.000	1.000	1.000
15	0.985	0.985	0.985	1.000	1.000	1.000
20	1.000	1.000	1.000	1.000	1.000	1.000

Table 4.2 shows that the situation for 5 particles is largely the same as for 4: Most of the overlaps are very high with 0.95 or above for the overlaps with the ground state and 0.99 or above among the CF candidates. The projection method which gives the highest overlap varies, with method 3 usually performing slightly worse than the others. For $L_b = 9$ method 3 actually gives the highest overlap, but not by all that much. There are two glaring and one not as glaring exceptions to this pattern: namely for $L_b = 11$, 13 and 14. Here the overlap with the ground state is much worse: 0.421 for $L_b = 11$, 0.803 for $L_b = 13$ and 0.256 for $L_b = 14$.

The square overlaps for these anomalies are 0.177, 0.645, 0.066, respectively. The $L_b = 13$ square overlap is respectable enough, at least it is well above 0.5 so the square overlap with all other eigenstates must be much smaller. But the $L_b = 11$ and 14 candidates fare much worse. The rest of the spectrum accounts for much more of the candidates than the ground state.

In all three of these low overlap cases, the overlaps among the CF candidates are all 1.000. So, from the perspective of evaluating method 3 compared with the well established methods 1 and 2, we cannot say based on these cases that method 3 is any worse than the others. Still it does show that our ground state candidates do not *always* give high overlaps with the true ground state. I will discuss these states further in a bit.

For 6 particles table 4.3 shows that again most overlaps with the ground state are very high. There are again a few exceptions, for some of which the overlap is so small that we should consider the states in question practically orthogonal. Still the overlaps among the CF candidates is very high. The one exception is $L = 8$, where the method

Table 4.3: Overlaps between the CF ground state candidates produced with projection methods 1, 2 and 3 and the exact ground state e for $N = 6$ particles. L is the bosonic angular momentum, related to total angular momentum as $L_{tot} = L + N(N-1)/2$.

L	$O(e,1)$	$O(e,2)$	$O(e,3)$	$O(1,2)$	$O(1,3)$	$O(2,3)$
0	1.000	1.000	1.000	1.000	1.000	1.000
2	1.000	1.000	1.000	1.000	1.000	1.000
3	1.000	1.000	1.000	1.000	1.000	1.000
4	1.000	0.999	0.989	0.999	0.989	0.995
5	0.993	0.996	0.965	1.000	0.989	0.985
6	0.991	0.994	0.966	1.000	0.992	0.988
7	0.961	0.958	0.963	1.000	1.000	0.999
8	0.997	0.991	0.984	0.992	0.983	0.996
9	0.982	0.978	0.948	1.000	0.986	0.985
10	0.973	0.967	0.949	1.000	0.994	0.994
11	0.944	0.943	0.938	1.000	0.985	0.982
12	0.910	0.911	0.862	0.999	0.991	0.990
13	0.178	0.188	0.200	1.000	0.999	1.000
14	0.949	0.946	0.953	1.000	0.996	0.996
15	0.979	0.973	0.970	1.000	0.998	0.998
16	0.179	0.151	0.055	0.998	0.987	0.991
17	0.160	0.158	0.148	1.000	0.992	0.991
18	0.942	0.942	0.926	1.000	0.997	0.997
20	0.988	0.987	0.989	1.000	1.000	0.999
21	0.723	0.728	0.728	0.988	0.988	1.000
22	0.043	0.043	0.043	1.000	1.000	1.000
23	0.322	0.322	0.322	1.000	1.000	1.000
24	0.986	0.986	0.986	1.000	1.000	1.000
30	1.000	1.000	1.000	1.000	1.000	1.000

3 candidate has an overlap of 0.504 with the method 1 candidate and 0.658 with the method 2 candidate. The overlap between the methods 1 and 2 candidates is high, at 0.979, so method 3 is the clear outlier here. Despite this, the overlap with the ground state is not so *that* much worse for candidate 3 than the other two, 0.814 for method 3, 0.877 for method 1 and 0.937 for method 2.

Just as for $N = 5$ method 3 typically has the lowest overlap with the ground state among the candidates, but again there are exceptions. This same pattern is repeated for $N = 7$ and $N = 8$ particles, except the typical overlap with the ground state, while still high, does seem to decrease as N increases.

Let us consider further the cases where the overlap with the ground state is less than $1/\sqrt{2}$ for at least one of the candidates, indicating that there "is" more of the rest of the spectrum in the candidate than there "is" of the ground state. In table 4.6 I have collected all candidates that have a higher overlap with any TI eigenstate other than the TI ground state than with the ground state. In all cases except for $N = 8, L = 33$, the candidates for all three projection methods have the highest overlap with the same

exact eigenstate. This is expected, as we have already seen that the candidates have very high overlaps with each other. We see that some of these states have a high overlap with the second lowest energy TI eigenstate, at 0.89 and above. However in many cases the highest overlap is quite low, lower than 0.8. Also in some cases the eigenstate with the highest overlap is as much as the 12th lowest energy eigenstate. When the maximal overlap is low the candidate states are not very similar to any particular eigenstate, but are superpositions of several high weight states. This is the case for the $N = 8, L = 33$ exception. There the method 1 candidate has overlap 0.496 with the ground state and 0.500 with the second lowest TI state. On the other hand the method 3 candidate has overlap 0.530 with the ground state and 0.489 with the second lowest state. The two candidates are almost identical with an overlap of 0.992, but the slight difference makes the maximal overlap state the ground state for the method 3 candidate and the second lowest state for the method 1 candidate.

There is one case where the overlap with the ground state is the maximal overlap, but still lower than $1/\sqrt{2}$, namely $N = 8, L = 43$. Here the overlap of the ground state and the method 1 candidate is 0.698, just below $1/\sqrt{2} \approx 0.707$, while overlap of the method 3 candidate with the ground state is 0.807. The second highest overlap of the method 1 candidate is with the tenth lowest TI eigenstate at 0.325. Other than this the overlaps are mostly quite low, lower than 0.2. For the method 3 candidate the ground state is the only state with an overlap higher than 0.2. This is a case where the overlap between the candidates is quite low at 0.763, but where the method 3 candidate has a significantly higher overlap with the ground state than the method 1 candidate.

Table 4.4: Overlaps between the CF ground state candidates produced with projection methods 1, 2 and 3 and the exact ground state e for $N = 7$ particles. L is the bosonic angular momentum, related to total angular momentum as $L_{tot} = L + N(N-1)/2$.

L	$O(e,1)$	$O(e,2)$	$O(e,3)$	$O(1,2)$	$O(1,3)$	$O(2,3)$
0	1.000	1.000	1.000	1.000	1.000	1.000
2	1.000	1.000	1.000	1.000	1.000	1.000
3	1.000	1.000	1.000	1.000	1.000	1.000
4	1.000	0.999	0.990	0.999	0.990	0.995
5	1.000	0.996	0.962	0.996	0.962	0.981
6	0.987	0.993	0.945	0.999	0.985	0.977
7	0.988	0.993	0.963	0.999	0.993	0.988
8	0.877	0.937	0.814	0.979	0.504	0.658
9	0.993	0.988	0.957	0.992	0.977	0.982
10	0.988	0.980	0.950	0.992	0.979	0.991
11	0.959	0.957	0.906	0.999	0.982	0.978
12	0.958	0.953	0.924	1.000	0.991	0.990
13	0.872	0.890	0.839	0.992	0.975	0.971
14	0.878	0.891	0.792	0.996	0.975	0.958
15	0.952	0.933	0.924	0.998	0.993	0.993
16	0.754	0.799	0.839	0.955	0.934	0.976
17	0.958	0.952	0.920	1.000	0.989	0.989
18	0.947	0.938	0.915	0.999	0.993	0.993
19	0.180	0.175	0.145	0.999	0.988	0.984
20	0.936	0.929	0.928	0.998	0.995	0.992
21	0.854	0.857	0.814	1.000	0.985	0.984
22	0.852	0.847	0.843	0.999	0.998	0.996
23	0.937	0.931	0.934	1.000	0.996	0.996
24	0.971	0.964	0.961	1.000	0.998	0.999
25	0.843	0.781	0.720	0.982	0.967	0.989
26	0.101	0.096	0.105	0.999	0.999	0.997
27	0.775	0.776	0.774	1.000	1.000	0.999
28	0.938	0.937	0.923	1.000	0.997	0.997
30	0.989	0.988	0.990	1.000	1.000	0.999
31	0.765	0.792	0.792	0.920	0.920	1.000
32	0.007	0.008	0.008	0.994	0.994	1.000
33	0.082	0.082	0.082	1.000	1.000	1.000
34	0.024	0.024	0.024	1.000	1.000	1.000
35	0.987	0.987	0.987	1.000	1.000	1.000
42	1.000	1.000	1.000	1.000	1.000	1.000

Table 4.5: Overlaps between the CF ground state candidates produced with projection methods 1 and 3 and the exact ground state e for $N = 8$ particles. L is the bosonic angular momentum, related to total angular momentum as $L_{tot} = L + N(N-1)/2$.

L	$O(e,1)$	$O(e,3)$	$O(1,3)$
0	1.000	1.000	1.000
2	1.000	1.000	1.000
3	1.000	1.000	1.000
4	1.000	0.991	0.991
5	1.000	0.961	0.961
6	0.999	0.933	0.936
7	0.981	0.934	0.985
8	0.986	0.965	0.995
9	0.991	0.930	0.896
10	1.000	0.950	0.950
11	0.974	0.905	0.975
12	0.975	0.908	0.962
13	0.943	0.889	0.984
14	0.946	0.907	0.988
15	0.979	0.936	0.962
16	0.873	0.844	0.981
17	0.932	0.881	0.986
18	0.920	0.872	0.988
19	0.944	0.823	0.917
20	0.318	0.377	0.986
21	0.903	0.852	0.989
22	0.312	0.350	0.963
23	0.908	0.863	0.982
24	0.936	0.901	0.992
25	0.547	0.518	0.994
26	0.814	0.792	0.994
27	0.875	0.802	0.985
28	0.920	0.885	0.992
29	0.014	0.015	0.996
30	0.947	0.935	0.996
31	0.432	0.419	0.996
32	0.901	0.894	0.998
33	0.496	0.530	0.992
34	0.608	0.603	0.996
35	0.959	0.949	0.998
36	0.197	0.202	0.999
37	0.036	0.029	0.966
38	0.893	0.893	1.000
39	0.089	0.092	0.993
40	0.933	0.919	0.997
42	0.986	0.986	1.000
43	0.698	0.807	0.763

Table 4.6: CF ground state candidates where the highest overlap is not with the TI ground state, but any other TI eigenstate. The state number is counted among the TI eigenstates from the lowest energy and up. N is the number of particles, L is the bosonic angular momentum, O is the overlap.

		method 1		method 2		method 3	
N	L	State	O	State	O	State	O
5	11	2	0.793	2	0.793	2	0.793
	14	2	0.951	2	0.951	2	0.951
6	13	2	0.938	2	0.938	2	0.937
	16	2	0.937	2	0.936	2	0.932
	17	2	0.929	2	0.927	2	0.930
	22	4	0.642	4	0.642	4	0.642
	23	3	0.795	3	0.795	3	0.795
7	19	3	0.756	3	0.758	3	0.742
	26	9	0.467	9	0.472	9	0.461
	32	2	0.722	2	0.718	2	0.718
	33	5	0.471	5	0.471	5	0.471
	34	3	0.512	3	0.512	3	0.512
8	20	2	0.896	-	-	2	0.843
	22	3	0.781	-	-	3	0.739
	25	3	0.721	-	-	3	0.723
	29	4	0.454	-	-	4	0.495
	31	3	0.597	-	-	3	0.590
	33	2	0.500	-	-	1	0.530
	34	2	0.711	-	-	2	0.702
	36	12	0.533	-	-	12	0.534
	37	2	0.695	-	-	2	0.554
	39	8	0.548	-	-	8	0.531

4.1.2 Energy Spectra

A different way to compare the CF candidates to the ground state is to directly compare the interaction energy of the candidates to the ground energy. This is useful because a candidate may have an energy very close to or even identical to the ground state energy and still have a low or even zero overlap.

In figures 4.1 – 4.5 I display the spectra of the $\nabla^2\delta$ interaction, together with the energies of the CF ground state candidates for $N = 4$–8 particles. As a sanity check we can see that each TI eigenvalue (marked by orange dots) is indeed repeated for higher Ls by COM excitations (gray dashes).

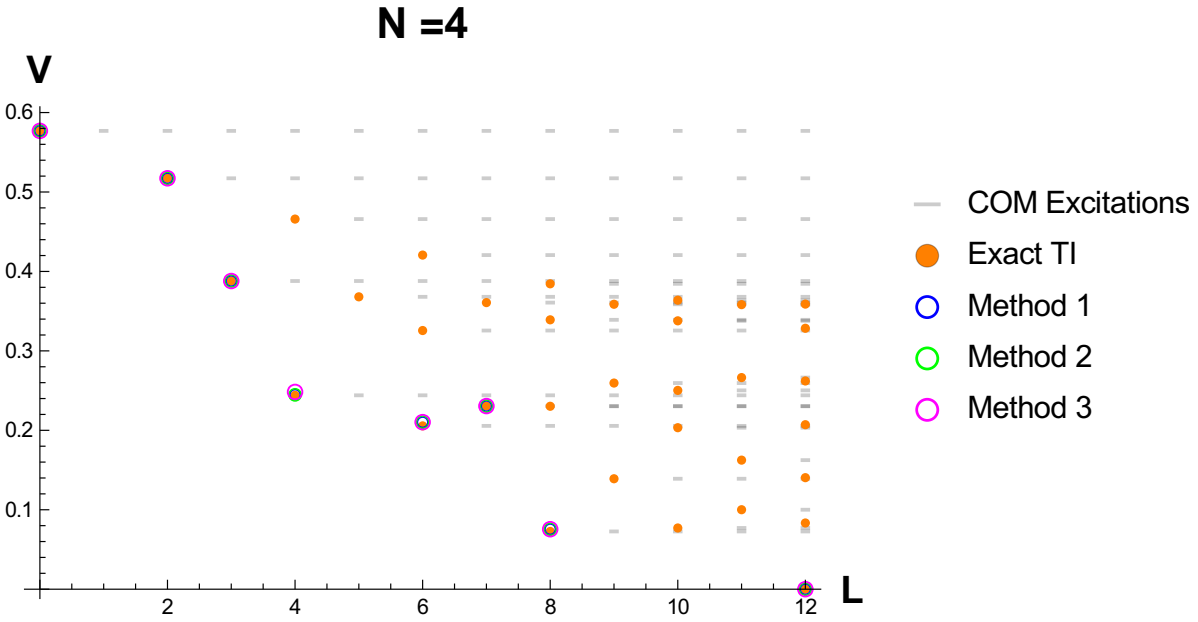

Figure 4.1: Energy spectrum of the $\nabla^2\delta$ interaction for 4 particles, and different values of L, the bosonic angular momentum, which is related to the total angular momentum as $L_{tot} = L + N(N-1)/2$. The orange dots and gray dashes are the eigenenergies of the translationally invariant states and the center of mass excitations, respectively, computed by exact diagonalization. The colored rings are the ground state energies of the interaction in the subspace spanned by minimal cyclotron energy compact states projected by the different methods.

Unsurprisingly, in the cases with high overlaps between the TI ground state and the CF candidates the energy is also very similar. They are, of course, slightly higher when they are not exactly the same, and just as the overlaps were mostly a little bit lower for method 3 than the other candidates, the energy seems to be a little bit higher for method 3.

The cases where the overlaps between the CF candidates and the exact TI ground state were low are reproduced in these plots as cases where the CF candidate energy is notably higher than that of the exact TI grounds state. We first note that in most cases the energy is still very close to the ground energy. Notable exceptions are $N = 7$ $L = 26$ and $N = 8$ $L = 29$, where the differences are of the order $0.1g$.

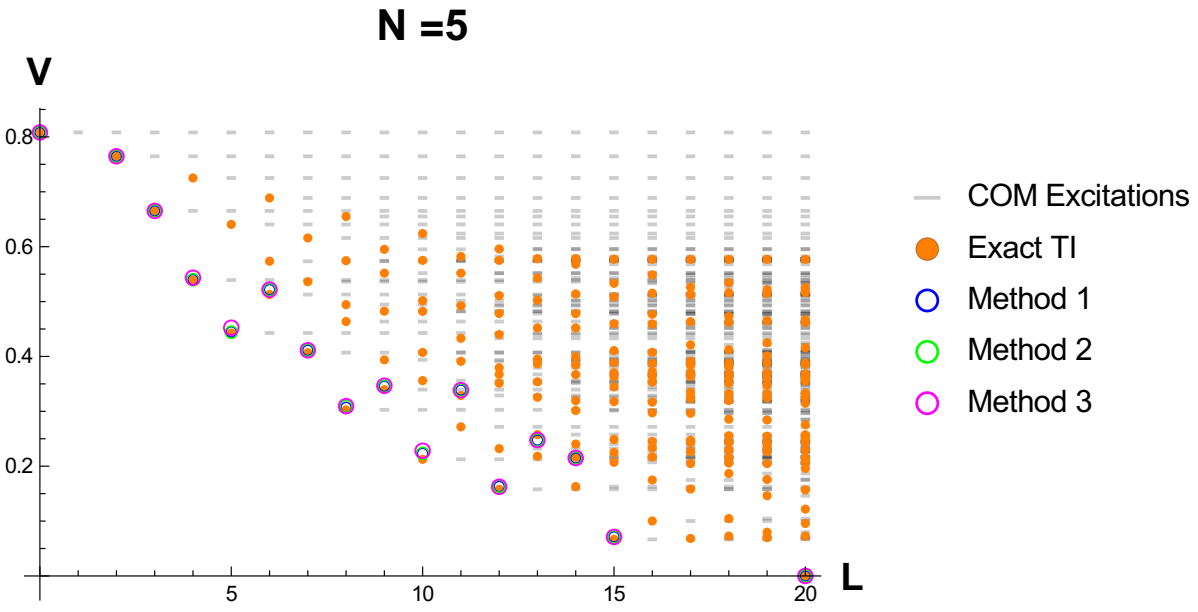

Figure 4.2: See figure 4.1 for explanation.

We see that in certain cases the ground state is not a TI state, but rather a COM excitation of a lower L TI state. These special TI states whose excitations are ground states are called a cusp states because of the shape they form on spectrum plots. We may call the cases accessible by compact states where the ground state is an excitation the post cusp cases. I have listed all cusp and post cusp states in table 4.7. Almost all cases where the CF candidates have low overlap with the ground state or the energy is clearly above the TI ground energy are post cusp states. On the other hand all cusp states have high overlaps and low energies. This holds for all projection methods, apparently the CF candidates are particularly bad at finding the TI ground state in post cusp cases.

I considered that this may be due to restricting the CF candidates to the lowest cyclotron energy states, and diagonalized the entire compact state space for projection method 3. This did not yield any improvement, and I concluded that the constraint was well founded and that this cusp problem is a property of compact states in general, and not only minimal cyclotron energy compact states.

While it would certainly be nice if CF states could provide good ground state candidates for post cusp cases, it is worth pointing out that the post cusp cases are precisely those where the true ground state is *not* TI and therefore cannot be found by compact states anyway. Since CF candidates are good approximations of the cusp states, we can find good approximations of post cusp ground state by exciting the CF cusp candidates.

Just as with the overlaps it does seem to be a trend that as N increases, the agreement between the exact ground state energy and the CF candidate energies decreases. We see this most clearly in figure 4.5, where almost all of the CF energies are clearly above the exact ones. This is just to be expected, as the dimensionality of the TI subspace grows it becomes harder and harder to "hit" the ground state with a guess. And the energies are after all still quite low and the overlaps quite high.

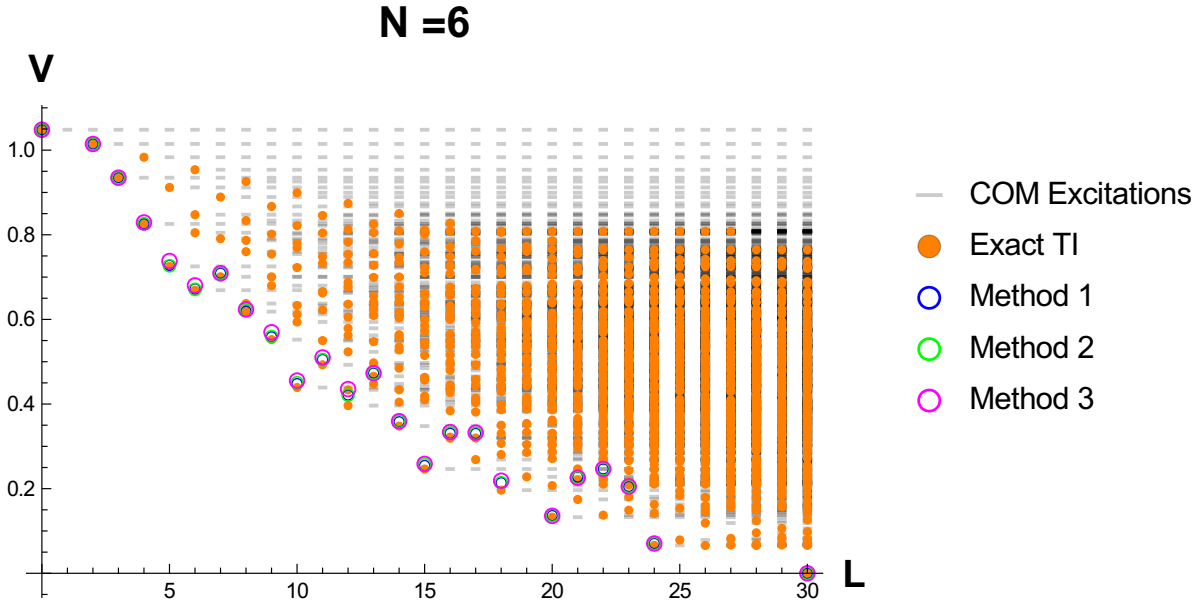

Figure 4.3: See figure 4.1 for explanation.

Table 4.7: List of cusp states and post cusp states accessible by compact states, listed by identifiers N and L.

N	cusp state Ls	post cusp state Ls
4	4, 6, 8, 12	7
5	5, 8, 10, 12, 15	6, 9, 11, 13, 14, 20
6	6, 10, 12, 15, 18, 20, 24, 30	7, 11, 13, 16, 17, 21, 22, 23
7	7, 12, 15, 18, 20, 24, 28, 30, 35, 42	8, 13, 19, 21, 25, 26, 27, 31, 32, 33, 34
8	14, 18, 21, 24, 26, 28, 30, 32, 35, 38, 40	15, 19, 22, 25, 27, 29, 31, 33, 36, 37, 39

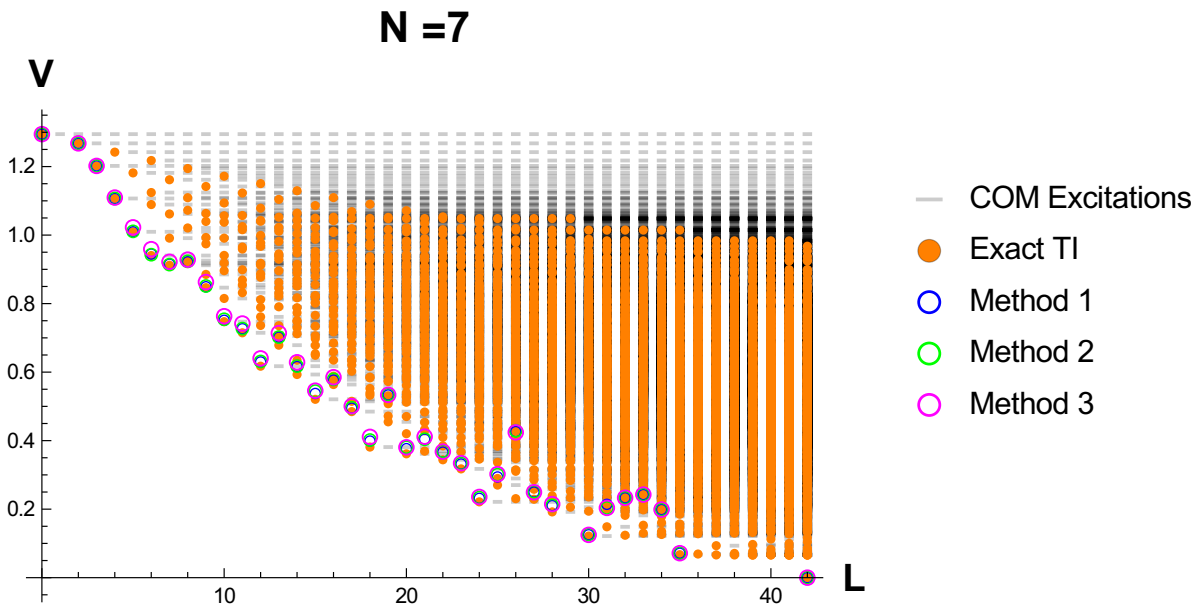

Figure 4.4: See figure 4.1 for explanation.

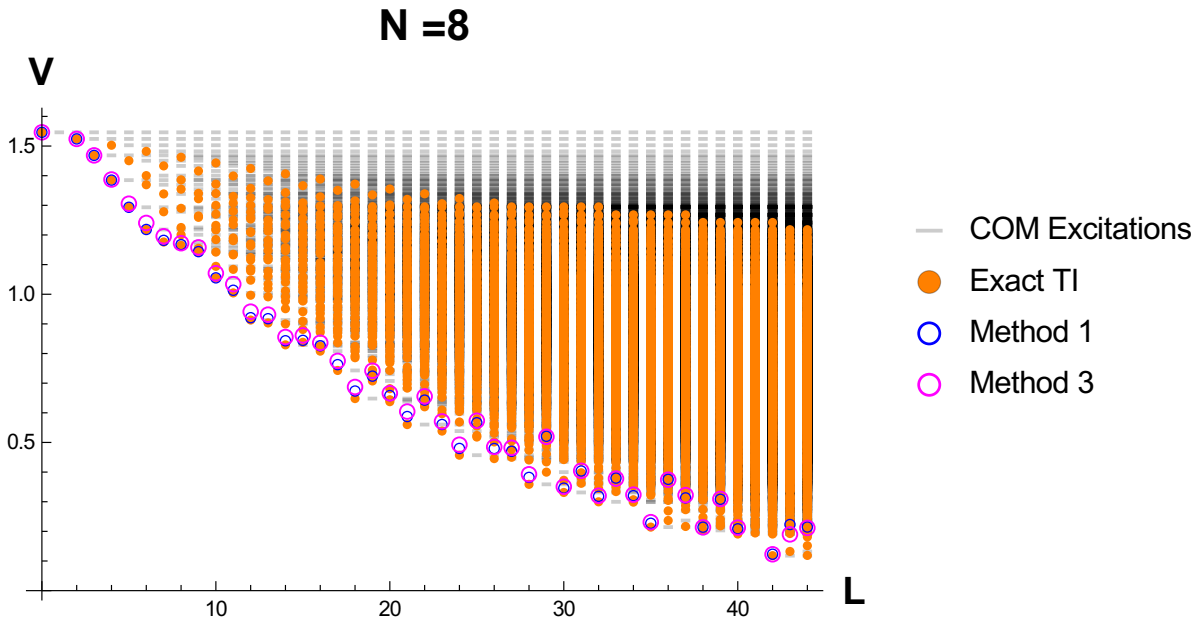

Figure 4.5: See figure 4.1 for explanation.

4.2 Linear Dependencies

Here I consider linear dependencies among projected CF determinants. The states considered here are not the ground state candidates from the previous section, as these were produced by diagonalizing the interaction in the space spanned by the states considered here. I will first look at the number of independent states both before projection and after projection by all three methods in section 4.2.1. Then I check for approximate linear dependencies and consider a few detailed examples in sections 4.2.2 and 4.2.3.

4.2.1 Number of Independent States

Figures 4.6 – 4.10 show the number of elements in the set of minimal cyclotron energy compact determinants $\{\Phi^C_{min}\}$ together with the number of strictly independent states after projection by all three methods. We see that in many cases there is only one determinant in $\left\{\Phi^C_{min,N,L}\right\}$ to begin with, which obviously means that there are no potential linear dependencies to discover. In some other cases all projection methods have reduced the number of independent states to 1, indicating that all of the determinants were equal up to normalization for all projection methods.

The most interesting cases though, are the ones where at least one of the projection methods give 2 or more independent states. In these cases projection methods 2 and 3 always give the same number of independent states, while method 1 sometimes gives the same number as the other two methods and sometimes more independent states than the others.

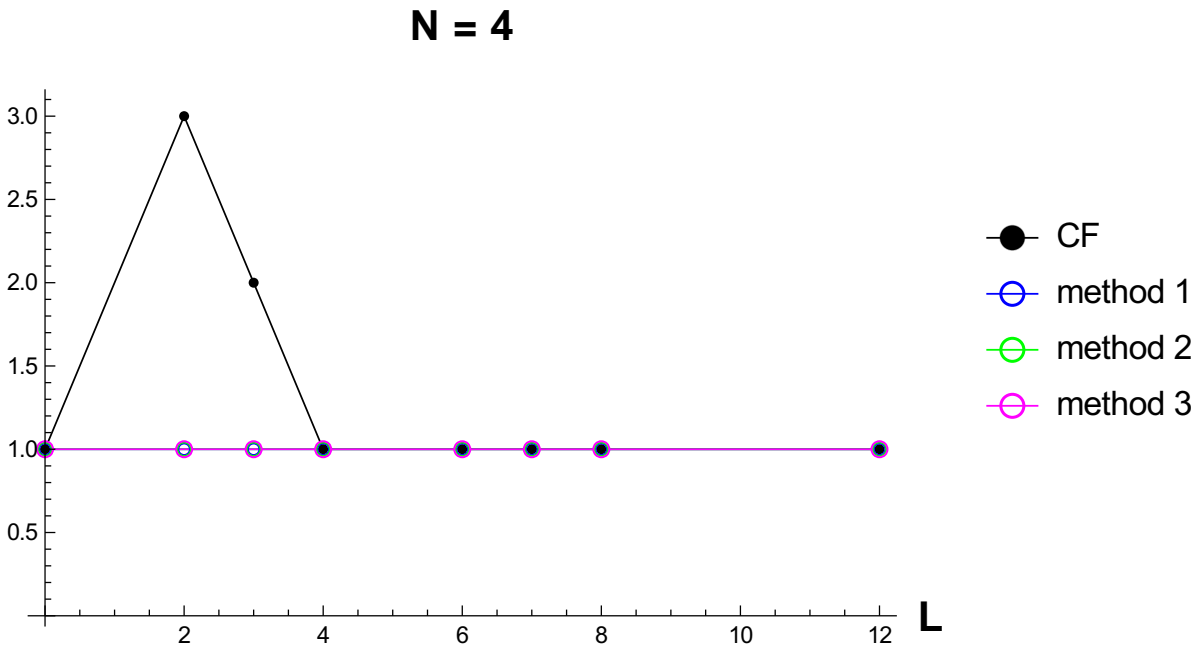

Figure 4.6: The number of independent states before and after projection for all projection methods, with 4 particles. L, the bosonic angular momentum, is related to the total angular momentum as $L_{tot} = L + N(N-1)/2$. The black dots are the number of different determinants in $\left\{\Phi^{C}_{min,N,L}\right\}$, while the colored rings are the number of strictly independent states after projection with the different methods.

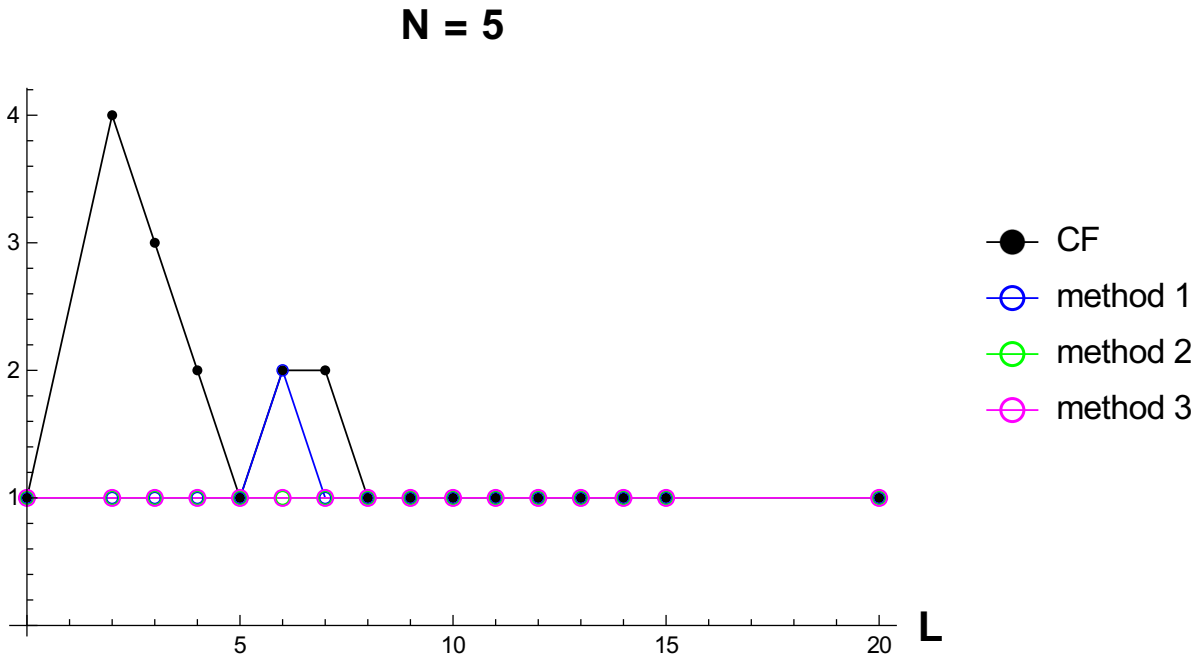

Figure 4.7: See figure 4.6 for explanation.

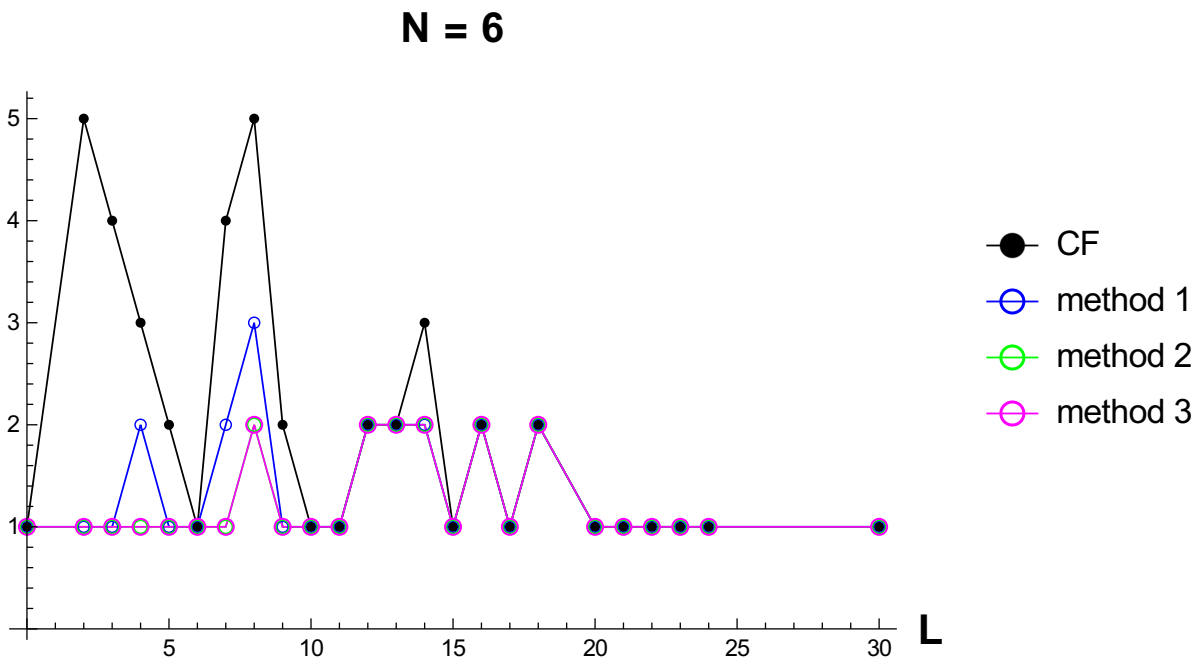

Figure 4.8: See figure 4.6 for explanation.

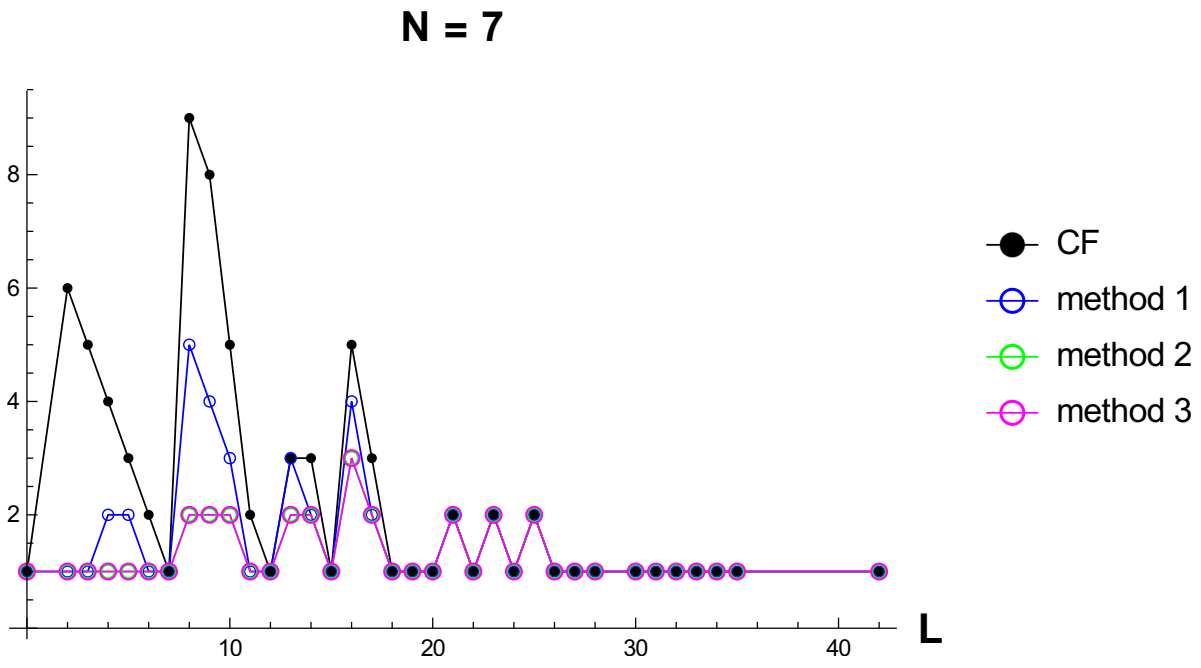

Figure 4.9: See figure 4.6 for explanation.

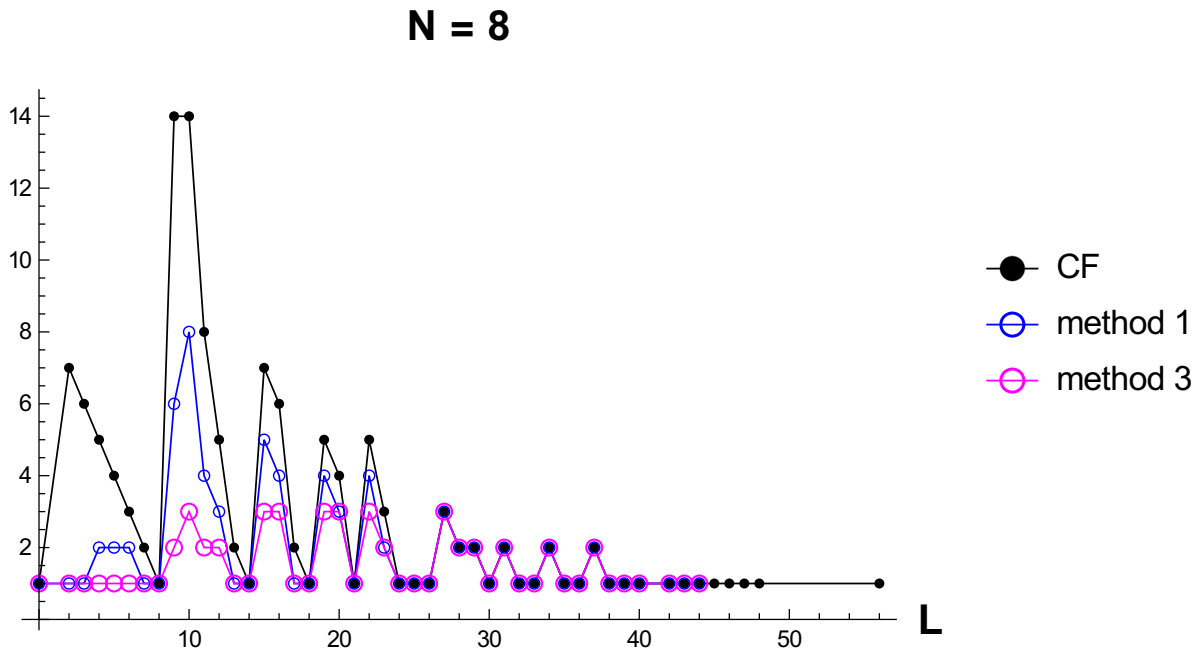

Figure 4.10: See figure 4.6 for explanation.

4.2.2 Approximate Linear Dependencies

If we allow for approximate linear dependencies the difference in the number of independent states for the different projection methods disappears. To see this consider table 4.8. There I have collected the number of non-zero singular values and the maximal relative difference between these singular values $\Delta = \max((\sigma_i - \sigma_{i+1})/\sigma_{i+1})$. If this measure is large it indicates a substantial gap in singular values. The smallest Δ for a case where there are more strictly independent states by method 1 than the others is 70.3 while the largest Δ for a case where there is already no difference is 1.52. Obviously there is no exact value for Δ that demarcates linear independence from approximate linear dependence. Still the gap between 70.3 and 1.52 is great enough that I think it is fair to say that the cases where method 1 gives more independent states than methods 2 and 3 are exactly the cases where there is approximate linear dependence in the method 1 set. The Δs for methods 2 and 3 are always lower than 1.52, so there is no approximate linear dependence there.

Table 4.8: The number of non-zero singular values # and the maximal relative difference $\Delta = \max((\sigma_i - \sigma_{i+1})/\sigma_{i+1})$ for all cases where $\# > 1$ for at least one projection method.

		method 1		method 2		method 3	
N	L	#	Δ	#	Δ	#	Δ
5	6	2	84.5	1	-	1	-
6	4	2	198	1	-	1	-
	7	2	85.4	1	-	1	-
	8	3	95.3	2	0.0907	2	0.324
	12	2	0.0446	2	0.032	2	0.274
	13	2	0.645	2	0.542	2	0.699
	14	2	0.464	2	0.396	2	0.498
	16	2	0.37	2	0.373	2	0.491
	18	2	0.205	2	0.193	2	0.236
7	4	2	113	1	-	1	-
	5	2	143	1	-	1	-
	8	5	1.25e+03	2	0.16	2	0.34
	9	4	214	2	0.0864	2	0.479
	10	3	83.9	2	0.0864	2	0.403
	13	3	102	2	0.415	2	0.482
	14	2	0.427	2	0.42	2	0.75
	16	4	104	3	0.839	3	1.07
	17	2	0.495	2	0.404	2	0.543
	21	2	0.318	2	0.292	2	0.362
	23	2	1.47	2	1.31	2	1.14
	25	2	0.337	2	0.482	2	0.601
8	4	2	99	-	-	1	-
	5	2	70.3	-	-	1	-
	6	2	143	-	-	1	-
	9	6	1.5e+03	-	-	2	0.444
	10	8	7.7e+04	-	-	3	0.783
	11	4	147	-	-	2	0.613
	12	3	77.6	-	-	2	0.465
	15	5	149	-	-	3	1.08
	16	4	77.9	-	-	3	1.14
	19	4	92.5	-	-	3	1.15
	20	3	0.559	-	-	3	0.863
	22	4	80.7	-	-	3	0.587
	23	2	0.333	-	-	2	0.353
	27	3	1.52	-	-	3	1.43
	28	2	0.105	-	-	2	0.0456
	29	2	0.206	-	-	2	0.244
	31	2	0.541	-	-	2	0.704
	34	2	1.12	-	-	2	0.856
	37	2	0.452	-	-	2	0.642

4.2.3 Some Detailed Examples

Let us look more closely at a few examples: A simple example of approximate linear dependence is the $N = 6, L = 4$ case. From figure 4.8 we see that there are three determinants in $\left\{\Phi^C_{min,6,4}\right\}$, two strictly independent states from method 1 and one independent state from methods 2 and 3. In table 4.9 we see from the reduced row echelon forms that projection methods 2 and 3 project all determinants to the same state, while method 1 gives two identical states and a third, different, state. However, we can tell by the low singular value that the third state is almost identical to the other two. So, if we consider approximately equal states equal, there is only one state even for method 1.

Table 4.9: Linear dependencies among the ground state candidates.

N = 6, L = 4		
Determinants		
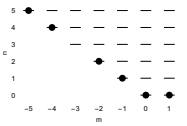	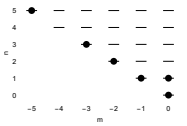	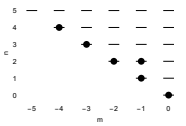
Reduced Row Echelon Form		
method 1 $\begin{bmatrix}1&0&0\\0&1&1\\0&0&0\end{bmatrix}$	method 2 $\begin{bmatrix}1&1&1\\0&0&0\\0&0&0\end{bmatrix}$	method 3 $\begin{bmatrix}1&1&1\\0&0&0\\0&0&0\end{bmatrix}$
Singular Values		
method 1 $\begin{bmatrix}1.73 & 0.0087\end{bmatrix}$	method 2 $\begin{bmatrix}1.73\end{bmatrix}$	method 3 $\begin{bmatrix}1.73\end{bmatrix}$

For a more complex example we can look at $N = 7, L = 8$ in table 4.10. Here there are nine determinants in $\left\{\Phi^C_{min,7,8}\right\}$. Projected by method 1 there are five independent states, while the four next may be written as four slightly different linear combinations of the five first. By contrast both methods 2 and 3 give three sets of identical states. States number 1,5 and 9 are identical, states number 2, 4, 6 and 8 are identical and states number 3 and 7 are identical. For both methods the states number 3 and 7 may be written as a linear combination of the other two states, though with different coefficients. The three extra independent states from method 1 correspond to three singular values "below the gap", that is to say three singular values that are much smaller than the other two, indicating that the extra states are really approximately linearly dependent on the two first.

As a final example consider $N = 8, L = 9$ in 4.11. Here there are fourteen determinants in $\left\{\Phi^C_{min,8,9}\right\}$. By method 1 there are now six independent states, while the next six are slightly different linear combinations and the final two are identical linear combinations. I do not have results for method 2 here, but method 3 again gives

Table 4.10: Linear dependencies among the ground state candidates.

N = 7, L = 8

Determinants

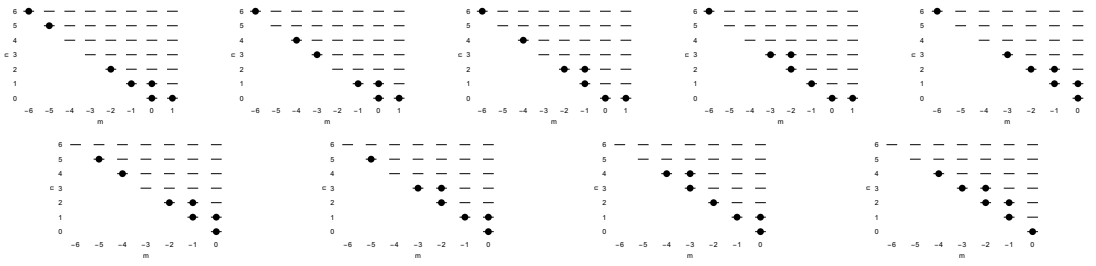

Reduced Row Echelon Form

method 1

$$\begin{bmatrix} 1 & 0 & 0 & 0 & 0 & -1.02 & -0.902 & -0.93 & -0.0498 \\ 0 & 1 & 0 & 0 & 0 & -0.424 & -0.374 & -0.286 & -0.12 \\ 0 & 0 & 1 & 0 & 0 & 2.23 & 1.97 & 2.1 & 0.0439 \\ 0 & 0 & 0 & 1 & 0 & -0.697 & -0.615 & -0.722 & 0.0536 \\ 0 & 0 & 0 & 0 & 1 & -0.795 & 0.177 & -0.825 & 1.01 \end{bmatrix}$$

method 2

$$\begin{bmatrix} 1 & 0 & 0.794 & 0 & 1 & 0 & 0.794 & 0 & 1 \\ 0 & 1 & 0.905 & 1 & 0 & 1 & 0.905 & 1 & 0 \\ 0 & 0 & 0 & 0 & 0 & 0 & 0 & 0 & 0 \\ 0 & 0 & 0 & 0 & 0 & 0 & 0 & 0 & 0 \\ 0 & 0 & 0 & 0 & 0 & 0 & 0 & 0 & 0 \end{bmatrix}$$

method 3

$$\begin{bmatrix} 1 & 0 & 1.23 & 0 & 1 & 0 & 1.23 & 0 & 1 \\ 0 & 1 & 1.12 & 1 & 0 & 1 & 1.12 & 1 & 0 \\ 0 & 0 & 0 & 0 & 0 & 0 & 0 & 0 & 0 \\ 0 & 0 & 0 & 0 & 0 & 0 & 0 & 0 & 0 \\ 0 & 0 & 0 & 0 & 0 & 0 & 0 & 0 & 0 \end{bmatrix}$$

Singular Values

method 1

$$\begin{bmatrix} 2.27 & 1.96 & 0.0323 & 0.0172 & 0.00182 \end{bmatrix}$$

method 2

$$\begin{bmatrix} 2.27 & 1.96 \end{bmatrix}$$

method 3

$$\begin{bmatrix} 2.4 & 1.79 \end{bmatrix}$$

two independent states, with states 3, 7, 9, 13 and 14 identical to the first, 6, 8 and 12 identical to the second and 4, 5, 10 and 11 identical linear combinations of the two first states. Just as in the last example all of the extra singular values for method 1 are "below the gap", so all of the extra linearly independent states may be considered as approximately linearly dependent on the first two.

In every case I have tested there are small singular values corresponding to every "extra" linearly independent state when projected by method 1 compared to methods 2 and 3. So if we were to eliminate all the approximate linear dependencies there would be the same number of linearly independent states. I have checked that for all examined cases the independent states are the same states as for methods 2 and 3. Meaning that if we can identify the determinants needed to form a basis for one method and are treating approximate linear dependencies as proper linear dependencies, those same determinants also form a basis for the two other projection methods.

This holds for the examined cases, that is to say the lowest cyclotron energy compact one species states for $N = 4 - 8$ particles. I expect it to hold also for higher N.

I have executed the algorithm for reducing linear dependencies outlined in section 3.9. The algorithm gave bases that are consistent with the linear dependencies or approximate linear dependencies found directly (as it had to). So the algorithm may perfectly well be applied to fermions, both projected by method 3, but also by the other two projection methods so long as the patterns found here hold for higher N.

Table 4.11: Linear dependencies among the ground state candidates.

N = 8, L = 9

Determinants

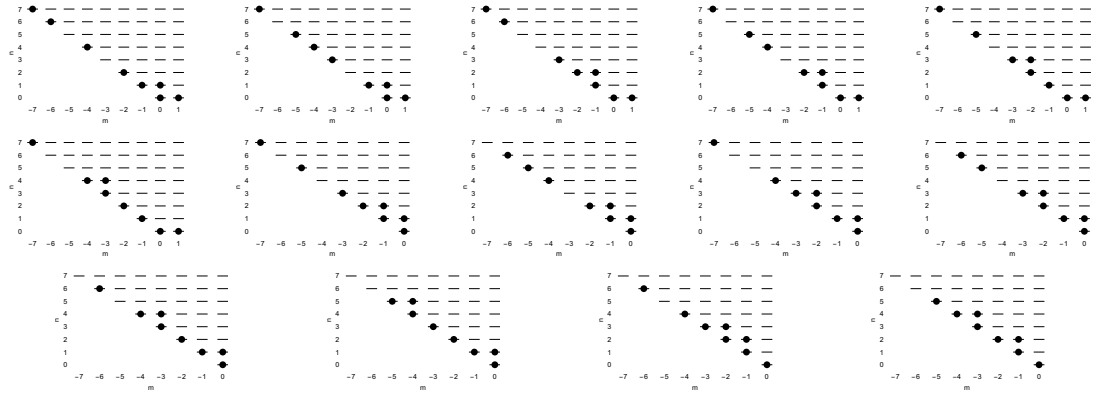

Reduced Row Echelon Form

method 1

$$\begin{bmatrix} 1 & 0 & 0 & 0 & 0 & 0 & -0.0209 & -0.97 & 0.196 & -1 & -0.764 & -0.647 & -0.0711 & -0.0711 \\ 0 & 1 & 0 & 0 & 0 & 0 & -1.13 & 0.38 & -1.03 & -0.471 & -0.322 & 0.619 & -1.19 & -1.19 \\ 0 & 0 & 1 & 0 & 0 & 0 & -1.37 & 1.96 & -1.96 & 0.946 & 0.661 & 1.85 & -1.62 & -1.62 \\ 0 & 0 & 0 & 1 & 0 & 0 & 1.43 & 0.905 & 0.8 & 2 & 1.52 & 0.375 & 1.33 & 1.33 \\ 0 & 0 & 0 & 0 & 1 & 0 & 1.8 & -2.07 & 2.81 & -0.725 & -0.253 & -1.95 & 2.23 & 2.23 \\ 0 & 0 & 0 & 0 & 0 & 1 & -2.24 & 1.73 & -2.72 & 0.0509 & -0.0537 & 1.92 & -2.57 & -2.57 \end{bmatrix}$$

method 3

$$\begin{bmatrix} 1 & 0 & 1 & 0.97 & 0.97 & 0 & 1 & 0 & 1 & 0.97 & 0.97 & 0 & 1 & 1 \\ 0 & 1 & 0 & 1.43 & 1.43 & 1 & 0 & 1 & 0 & 1.43 & 1.43 & 1 & 0 & 0 \\ 0 & 0 & 0 & 0 & 0 & 0 & 0 & 0 & 0 & 0 & 0 & 0 & 0 & 0 \\ 0 & 0 & 0 & 0 & 0 & 0 & 0 & 0 & 0 & 0 & 0 & 0 & 0 & 0 \\ 0 & 0 & 0 & 0 & 0 & 0 & 0 & 0 & 0 & 0 & 0 & 0 & 0 & 0 \end{bmatrix}$$

Singular Values

method 1

$$\begin{bmatrix} 2.73 & 2.56 & 0.048 & 0.0212 & 0.0148 & 0.00182 \end{bmatrix}$$

method 3

$$\begin{bmatrix} 3.08 & 2.13 \end{bmatrix}$$

Chapter 5

Conclusion and Outlook

5.1 Summary and Conclusions

In this thesis I have investigated a new method for projecting composite fermion Slater determinants to the lowest Landau level, called method 3. The method is based on attaching a Jastrow factor to a bosonic wave function projected by the standard projection method 1.

We want to know how well projection method 3 works. I have compared the method 3 CF ground state candidate to both the exact ground state from a numerical diagonalization and to the ground state candidates for projection methods 1 and 2. As found in chapter 4 the overlap among the CF candidate states is almost uniformly very high. As N grows the overlap among candidates decreases slightly, but remains high. The energies of the different candidates are also very similar. This indicates that projection method 3 works about as well as the other methods.

Similarly, the overlaps of all the CF candidates with the TI ground state is typically very high, with method 3 typically performing slightly worse than the other methods. This overlap also decreases with N. Typically the CF energies are also very close to the true TI ground state energies, although they grow apart with N. There are, however, exceptions. I found that almost all cases where the overlap with the TI ground state is low, or the CF energy is very different from the TI ground state energy is in so-called post cusp cases. These are values of L where the true ground state is not TI, but rather a center of mass excitation of a lower L TI state, called a cusp state. The CF candidates provide good approximations of the cusp states, so the true ground state in post cusp cases may be well approximated by exciting a cusp state candidate.

All in all it seems that projection method 3 gives quite good approximations of the ground state, and a very similar approximation to other CF projection methods.

The other main topic of this thesis has been the linear dependencies of projected CF states. I have compared the linear dependencies among CF wave functions found by projecting the minimal cyclotron energy compact states for a given N and L. For all tested cases ($N = 4$ - 8 and Ls up to 44) methods 2 and 3 give the "same" linear dependencies, in the sense that same coefficients are non-zero, though they have different values. On the other hand method 1 often gives different linear dependencies, with more linearly independent states than for the other two methods. This difference is resolved by considering approximate linear dependencies. Then the linear dependen-

cies from method 1 are reduced to those for methods 2 and 3. So in this sense all three projection methods give the same linear dependencies. In particular, if one could identify a set of determinants that when projected will be a basis for the space of minimal cyclotron energy compact states for one of the methods, the same determinants form a basis (or approximate basis in the case of method 1) for the other methods. Such a basis can be found, at least for up to 12 particles, with the procedure outlined in [8].

5.2 Open Questions and Outlook

There are several pertinent questions about projection method 3 that are left unanswered by this thesis. Most obviously, it would be good to find the exact ground state of the $\nabla^2\delta$ interaction for more than eight particles and check how well the method 3 CF ground state candidate compares. It may also be interesting to see if changing the interaction significantly alters the results, for example by using the Coulomb interaction.

Next it should be checked how well method 3 performs for more than one species of particles, especially for simple states. If it does similarly as for few particles of one species, then the basis from [8, 9, 10] may be immediately applied to fermions to find a good approximation of the low energy spectrum.

Similarly it should be checked whether the linear dependencies among method 1 and 2 projected states remain equal or approximately equal to the linear dependencies among the method 3 projected states for more than one species, or for compact states that are not minimal in cyclotron energy.

The point of investigating projection method 3 was to learn more about the linear dependency puzzle for fermionic CF wave functions. In this thesis I have shown that finding results for bosonic CF wave functions and importing them to the fermionic case works well enough for single species low energy compact states that I expect it to also work for other cases. Hopefully it will be possible to extend the work on bosonic compact state linear dependencies into a proper basis for all compact states, with any cyclotron energy and any number of species. If that happens the results may be imported to the fermionic case by method 3 and hopefully will also hold for methods 1 and 2. That would explain why the linear dependencies that show up show up and thus resolve the linear dependency puzzle for compact states, at least from the mathematical perspective. For the realist about CFs it would provide a kind of explanation of why the interaction from [7] has the form that it has, although it does not exactly provide a physical explanation for why such an interaction should exist.

Appendices

Appendix A

Additional Calculations

A.1 The $\nabla^{2n}\delta$ Interaction for Bosons and Fermions

Consider a two-particle interaction on the form

$$v(z_i - z_j) = \sum_{n=0}^{\infty} v_n \nabla^{2n} \delta(z_i - z_j). \tag{A.1}$$

When the particles are close together we may expand the wavefunction in terms of $z = z_i - z_j$. For a bosonic wavefunction only even powers of z can contribute, due to symmetry:

$$\psi(z) = \sum_{n=0}^{\infty} c_{2n} z^{2n}, \tag{A.2}$$

and so

$$\langle v \rangle = \int d^2z \sum_{klm} v_m \bar{c}_{2k} c_{2l} \bar{z}^{2k} \left(\nabla^{2m} \delta(z) \right) z^{2l}. \tag{A.3}$$

Using

$$\nabla^2 = 4\partial\bar{\partial} \tag{A.4}$$

we find that each term in the sum over k, l, m is proportional to

$$\int d^2z \; \bar{z}^{2k} z^{2l} (\partial\bar{\partial})^m \delta(z). \tag{A.5}$$

By partial integration this is

$$\int d^2z \; \left((\partial\bar{\partial})^m \bar{z}^{2k} z^{2l} \right) \delta(z). \tag{A.6}$$

The factor $(\partial\bar{\partial})^m \bar{z}^{2k} z^{2l}$ is zero if $m > 2k$ or $m > 2l$, thus those terms don't contribute. If $m < 2k$ or $m < 2l$ the factor is a product of positive powers of z and $\bar{z}$, and the delta function makes the integral zero. So the only contribution is from terms with $m = 2k = 2l$, where our factor is the constant $((2k)!)^2$, which is also the value of the integral. Thus, for bosons only the terms with even m contribute.

If we instead look at fermionic wavefunctions only odd terms in z contribute to the wave function due to antisymmetry so the expansion (A.2) becomes instead

$$\psi(z) = \sum_{n=0}^{\infty} c_{2n+1} z^{2n+1}. \tag{A.7}$$

We find that a term in $\langle v \rangle$ is proportional to

$$\int d^2z \, \bar{z}^{2k+1} z^{2l+1} (\partial\bar{\partial})^m \delta(z), \tag{A.8}$$

the same arguments as above mean that the only non-zero terms are those where $m = 2k+1 = 2l+1$. Thus only odd m contribute for fermions.

We may now write

$$v_{bose} = \sum_{n=0}^{\infty} v_{2n} \nabla^{4n} \delta(z_i - z_j), \tag{A.9}$$

$$v_{fermi} = \sum_{n=0}^{\infty} v_{2n+1} \nabla^{4n+2} \delta(z_i - z_j). \tag{A.10}$$

Appendix B

Algorithms

B.1 Finding All Compact States with N particles

Here I detail the algorithm I used to find all compact states. A state may be represented as N integer pairs (n, m) with $n = 0, 1, \ldots$ and $m = -n, -n+1, \ldots$. Let $\left\{ \Phi_C^N \right\}$ be the set of compact state determinants with N particles.

The rules are: No gaps to the left, no gaps below, no particles with $n \geq N$
Let $\left\{ \Phi_C^1 \right\} = \{ (0,0) \}$
for $N^* = 1, 2, \ldots N-1$ **do**
  forall $x \in \left\{ \Phi_C^{N^*} \right\}$ **do**
    for $\lambda = \max(n \in x), \ldots, N^*$ **do**
      Let x^* be x with an added particle at leftmost unoccupied position of Λ level λ
      if *the rules hold for* x^* **then**
        Add x^* to $\left\{ \Phi_C^{N^*+1} \right\}$
      end
    end
  end
end
Remove all states from $\left\{ \Phi_C^N \right\}$ where $\sum_i m_i < -N(N-1)$

Algorithm 1: Algorithm for finding all compact states with N particles.

Then it is straightforward to pick out the minimal cyclotron energy subsets for each L, if needed.

B.2 Projection to the LLL

Here I collect the algorithm I used for performing the projections. All three algorithms give unantisymmetrized polynomials that can be cast into the monomial basis without antisymmetrizing. I have written them out as symbolic polynomials, but this is not necessary for implementation.

B.2.1 Method 1

Let N be the number of particles
Let $\boldsymbol{n}$ and $\boldsymbol{m}$ be the occupied n and m values of the determinant
$S := 0$ `// Projected state`
forall $\rho, \sigma \in S_N$ **do**
  $t_i := \rho(i) + \sigma(i) - 2$ `// The exponents of a term in` $\mathcal{J}^2$
  $d_i := \frac{t_i!}{(t_i - n_i)!}$
  $(-1)^{|t+m|} :=$ Signature of $\{ t_i + m_i \}$ compared to the sorted set
  $\boldsymbol{x} :=$ Sorted($\{ t_i + m_i \}$)
  if $\boldsymbol{x}$ *has no duplicates* **then**
    $S+ = (-1)^{|t+m|+|\rho|+|\sigma|} \prod_{i=1}^{N} d_i z_i^{x_i}$
  end
end

Algorithm 2: Algorithm for projecting a compact state to the LLL by method 1.

B.2.2 Method 2

Let N be the number of particles
Let $\boldsymbol{n}$ and $\boldsymbol{m}$ be the occupied n and m values of the determinant
$P_T := 1$
for $i = 1, 2, \ldots, N$ **do**
  $S_T := 0$
  for $k = 0, 1, \ldots, N - 1 - n_i$ **do**
    $f := \frac{(N-1-k)!}{(N-1-k-n_i)!}$
    if $f \neq 0$ **then**
      $e_k(\{ z \} \setminus z_i) :=$ the kth elementary symmetric polynomial of $\{ z \} \setminus z_i$
      $S_T+ = f z_i^{N-1-k+m_i} e_k(\{ z \} \setminus z_i)$
    end
  end
  $P_T\times = S_T$
end
Expand P_T
$S = 0$ `// Final state`
foreach *term* $\in P_T$ **do**
  $\boldsymbol{x} :=$ exponents of term
  $c :=$ coefficient of term
  if $\boldsymbol{x}$ *has no duplicates* **then**
    $S+ = (-1)^{|x|} c \prod_{i=1}^{N} z_i^{x_i}$
  end
end

Algorithm 3: Algorithm for projecting a compact state to the LLL by method 1.

B.2.3 Method 3

Let N be the number of particles
Let $\boldsymbol{n}$ and $\boldsymbol{m}$ be the occupied n and m values of the determinant
$S_B := 0$ `// Boson part of state`
forall $\rho \in S_N$ **do**
  $t_i := \rho(i) - 1$ `// The exponents of a term in` $\mathcal{J}$
  $d_i := \frac{t_i!}{(t_i - n_i)!}$
  if $\prod_{i=1}^{N} d_i \neq 0$ **then**
    $\boldsymbol{x} :=$ Sorted($\{ t_i + m_i \}$)
    $f_i :=$ Factorial of multiplicity of x_i in $\boldsymbol{x}$
    $S_B += (-1)^{|\rho|} \prod_{i=1}^{N} d_i f_i z_i^{x_i}$
  end
end
S = 0 `// Final state`
foreach *term* $\in S_B$ **do**
  $\boldsymbol{x} :=$ Exponents of term
  $c :=$ coefficient of term
  forall $\rho \in S_N$ **do**
    $\boldsymbol{t} :=$ Sorted($\left\{ x_{\rho(i)} + (i-1) \right\}$)
    if $\boldsymbol{t}$ *has no duplicates* **then**
      $S += (-1)^{|\boldsymbol{t}|} c \prod_{i=1}^{N} z_i^{t_i}$
    end
  end
end

Algorithm 4: Algorithm for projecting a compact state to the LLL by method 3.

Bibliography

[1] X.-G. Wen, "Colloquium: Zoo of quantum-topological phases of matter," *Rev. Mod. Phys.*, vol. 89, p. 041004, Dec 2017.

[2] C. Nayak, S. H. Simon, A. Stern, M. Freedman, and S. Das Sarma, "Non-abelian anyons and topological quantum computation," *Rev. Mod. Phys.*, vol. 80, pp. 1083–1159, Sep 2008.

[3] J. M. Leinaas and J. Myrheim, "On the theory of identical particles," *Il Nuovo Cimento B (1971-1996)*, vol. 37, pp. 1–23, Jan 1977.

[4] F. Wilczek, "Quantum mechanics of fractional-spin particles," *Phys. Rev. Lett.*, vol. 49, pp. 957–959, Oct 1982.

[5] N. Gemelke, E. Sarajlic, and S. Chu, "Rotating Few-body Atomic Systems in the Fractional Quantum Hall Regime," *ArXiv e-prints*, July 2010.

[6] X. G. Wu and J. K. Jain, "Excitation spectrum and collective modes of composite fermions," *Phys. Rev. B*, vol. 51, pp. 1752–1761, Jan 1995.

[7] A. C. Balram, A. Wójs, and J. K. Jain, "State counting for excited bands of the fractional quantum hall effect: Exclusion rules for bound excitons," *Phys. Rev. B*, vol. 88, p. 205312, Nov 2013.

[8] M. L. Meyer, O. Liabøtrø, and S. Viefers, "Linear dependencies between composite fermion states," *Journal of Physics A: Mathematical and Theoretical*, vol. 49, no. 39, p. 395201, 2016.

[9] O. Liabøtrø and M. L. Meyer, "Composite fermion basis for two-component bose gases," *Phys. Rev. A*, vol. 95, p. 033633, Mar 2017.

[10] V. Skogvoll and O. Liabøtrø, "Composite fermion basis for m -component bose gases," *Journal of Physics A: Mathematical and Theoretical*, vol. 50, no. 40, p. 405301, 2017.

[11] E. H. Hall, "On a new action of the magnet on electric currents," *American Journal of Mathematics*, vol. 2, no. 3, pp. 287–292, 1879.

[12] K. V. Klitzing, G. Dorda, and M. Pepper, "New Method for High-Accuracy Determination of the Fine-Structure Constant Based on Quantized Hall Resistance," *Physical Review Letters*, vol. 45, pp. 494–497, Aug. 1980.

[13] R. B. Laughlin, "Quantized hall conductivity in two dimensions," *Phys. Rev. B*, vol. 23, pp. 5632–5633, May 1981.

[14] D. C. Tsui, H. L. Stormer, and A. C. Gossard, "Two-dimensional magnetotransport in the extreme quantum limit," *Phys. Rev. Lett.*, vol. 48, pp. 1559–1562, May 1982.

[15] W. Pan, J. S. Xia, H. L. Stormer, D. C. Tsui, C. Vicente, E. D. Adams, N. S. Sullivan, L. N. Pfeiffer, K. W. Baldwin, and K. W. West, "Experimental studies of the fractional quantum hall effect in the first excited landau level," *Phys. Rev. B*, vol. 77, p. 075307, Feb 2008.

[16] R. B. Laughlin, "Anomalous quantum hall effect: An incompressible quantum fluid with fractionally charged excitations," *Phys. Rev. Lett.*, vol. 50, pp. 1395–1398, May 1983.

[17] J. K. Jain, "Composite-fermion approach for the fractional quantum hall effect," *Phys. Rev. Lett.*, vol. 63, pp. 199–202, Jul 1989.

[18] N. K. Wilkin, J. M. F. Gunn, and R. A. Smith, "Do attractive bosons condense?," *Phys. Rev. Lett.*, vol. 80, pp. 2265–2268, Mar 1998.

[19] S. Viefers, "Quantum hall physics in rotating bose–einstein condensates," *Journal of Physics: Condensed Matter*, vol. 20, no. 12, p. 123202, 2008.

[20] M. L. Meyer, "Rotational properties of two-component bose gases," Master's thesis, University of Oslo, 2013.

[21] V. Skogvoll, "Three m-species generalizations for rotating bose gases in the lowest landau level," Master's thesis, University of Oslo, 2017.

[22] J. K. Jain, *Composite Fermions*. Cambridge University Press, 2007.

[23] T. H. Hansson, M. Hermanns, S. H. Simon, and S. F. Viefers, "Quantum hall physics: Hierarchies and conformal field theory techniques," *Rev. Mod. Phys.*, vol. 89, p. 025005, May 2017.

[24] S. A. Trugman and S. Kivelson, "Exact results for the fractional quantum hall effect with general interactions," *Phys. Rev. B*, vol. 31, pp. 5280–5284, Apr 1985.

[25] S. M. Girvin and T. Jach, "Formalism for the quantum hall effect: Hilbert space of analytic functions," *Phys. Rev. B*, vol. 29, pp. 5617–5625, May 1984.

[26] T. Papenbrock and G. F. Bertsch, "Exact solutions for interacting boson systems under rotation," *Journal of Physics A: Mathematical and General*, vol. 34, no. 3, p. 603, 2001.

[27] M. L. Meyer, G. J. Sreejith, and S. Viefers, "Rotational properties of two-component bose gases in the lowest landau level," *Phys. Rev. A*, vol. 89, p. 043625, Apr 2014.

[28] V. Ruuska and M. Manninen, "Algebraic analysis of composite fermion wavefunctions," *Phys. Rev. B*, vol. 72, p. 153309, Oct 2005.

[29] M. Manninen, S. Viefers, M. Koskinen, and S. M. Reimann, "Many-body spectrum and particle localization in quantum dots and finite rotating bose condensates," *Phys. Rev. B*, vol. 64, p. 245322, Dec 2001.

[30] G. F. Bertsch and T. Papenbrock, "Yrast line for weakly interacting trapped bosons," *Phys. Rev. Lett.*, vol. 83, pp. 5412–5414, Dec 1999.

[31] H. Saarikoski, S. M. Reimann, A. Harju, and M. Manninen, "Vortices in quantum droplets: Analogies between boson and fermion systems," *Rev. Mod. Phys.*, vol. 82, pp. 2785–2834, Sep 2010.

[32] J. K. Jain and R. K. Kamilla, "Quantitative study of large composite-fermion systems," *Phys. Rev. B*, vol. 55, pp. R4895–R4898, Feb 1997.

[33] M. B. Nathanson, *Elementary Methods in Number Theory*. Springer, 2000.

[34] D. C. Lay, *Linear Algebra and Its Applications, 4th Edition*. Pearson, 2011.

[35] C. Jordan, "Mémoire sur les formes bilinéaires,," *Journal de Mathématiques Pures et Appliquées*, vol. 19, pp. 35–54, 1874.

[36] G. W. Stewart, "On the early history of the singular value decomposition," *SIAM Review*, vol. 35, no. 4, pp. 551–566, 1993.

[37] H. Weyl, "Das asymptotische verteilungsgesetz der eigenwerte linearer partieller differentialgleichungen (mit einer anwendung auf die theorie der hohlraumstrahlung)," *Mathematische Annalen*, vol. 71, pp. 441–479, 1912.